PREDICTION OF AMPLITUDE AND WAVELENGTH OF TROUGHS ON POLYETHYLENE WEBS

By

ADITYA GOTIMUKUL

Bachelor of Engineering in Mechanical Engineering

Jawaharlal Nehru Technological University

Hyderabad, Andhra Pradesh

2007

Submitted to the Faculty of the
Graduate College of the
Oklahoma State University
in partial fulfillment of
the requirements for
the Degree of
MASTER OF SCIENCE
May, 2010

PREDICTION OF AMPLITUDE AND WAVELENGTH

OF TROUGHS ON POLYETHYLENE WEBS

Thesis Approved:

Dr. J.K.Good

Thesis Adviser

Dr. Raman P. Singh

Dr. Sandip P. Harimkar

Dr. A. Gordon Emslie

Dean of the Graduate College

ACKNOWLEDGMENTS

First and foremost I would like to offer my sincere gratitude to Dr. J.K. Good for his support, guidance and every other thing he has done for me. I appreciate him for patiently guiding, helping, and supporting me in all situations through out my research work.

Secondly I would like to thank my committee members Dr. Raman P Singh and Dr. Sandip P. Harimkar for willing to be my committee member. I would like to sincerely extend my gratitude to Mr. Ron Markum for his invaluable help in developing the experimental setups and conducting experiments. I would also like to thank WHRC sponsors for funding my research and my friends at OSU for their help.

Last but not the least I would like to thank my parents Ashok Gotimukul, Usha Gotimukul and my sister Ajitha Gotimukul for there continuous emotional and financial support through out.

TABLE OF CONTENTS

LIST OF TABLES

LIST OF FIGURES

Figure Page

CHAPTER I

INTRODUCTION

Throughing of Webs:

A Web is a continuous thin strip of material, made of paper, plastic films, textiles and thin metals sheets. The webs often have to undergo several continuous processes prior to forming a final product. The transportation of these webs during web processes is known as web handling. Webs are often quite thin and such are subjected to instability. In the process machinery webs are supported intermittently by rollers. The unsupported web between the rollers is called free span.

During the transportation of webs, small out of plane deformations called troughs may appear in the free span of the web. Formation of troughs in free span, hinder the processes such as printing and coating etc due to non planar geometry in the web span. Also these troughs may results in wrinkles on the rollers, which cause serious degradation of material quality. The direction of travel of the web through a process machine is called the machine direction (MD). The direction orthogonal to the machine direction, but still in the plane of the web is called cross machine direction (CMD).

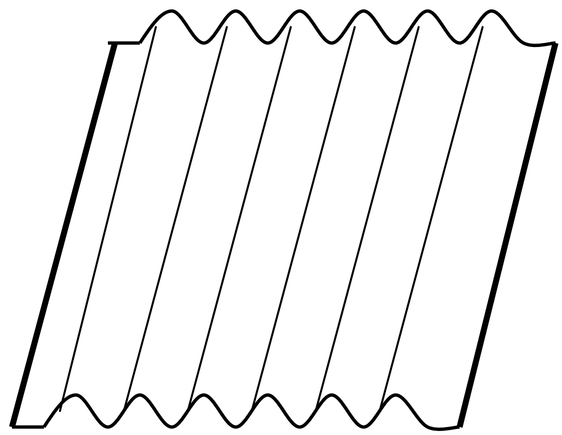

Figure 1.1-MD Trough Formation

Reasons for Troughing of Webs:

The troughs in the free span occur due to compressive stresses in CMD. A free body diagram of a web would show that there are no lateral forces at the edge of the web to create compressive stresses. However CMD compressive stresses can arise that result in trough formation for various reasons, some of which are:

a) Roller deflection: The deflection of the roller causes lateral compressive stress, as the web seeks to align itself perpendicular to the axis of the deflected roller.

b) Variation of tension: Tensile stress (σ_x) due to tension in a web causes web strain (ε_x) in the MD and web strain (ε_y) equal to ($-\nu\varepsilon_x$) in CMD. Longitudinal strain observed as the plastic films are processed in web form can be of the order of 0.001, although the strain increases and decreases during the process due to changes in tension. Changes in width accompany these changes in longitudinal tension due to Poisson's ratio which is of the order of 0.3 and larger. Therefore, an increase in width occurs when a web moves from high tension span to low tension span. Changes in web tensions must occur at rollers where the change in tension is balanced by frictional forces between the web and roller. As the web tension decreases the web attempts to expand laterally on the roller which can produce CMD compressive stress.

c) Increase in temperature or moisture: Plastic webs have a high coefficient of thermal expansion, in some cases higher than 0.0001 per degree F and paper usually expands significantly as it absorbs moisture. The processes such as drying and corona or flame treatment involve heating of webs. In the process called sizing, paper is made to absorb moisture. If lateral expansion of a web occurs near a roller, frictional CMD forces can arise between the web and roller which produce CMD compressive stresses, similar to the Poisson's effect discussed in case of variation of tension.

d) Viscoelastic memory: In draw or velocity controlled processes the web tension can decrease in-span due to viscoelasticity. Decrease tension will result in CMD expansion which can produce troughs.

e) Roller Imperfections: Both roller misalignment and roller diametrical taper are capable of producing roughs in the web.

Given the current understanding of the sources of the CMD forces which create troughs it is still difficult to make troughs disappear by attempting to control these sources.

The focus of this research is that if it is given that web troughs will occur can their amplitudes be predicted? The goal of this research is to quantify the wavelength and the amplitude of these troughs when MD web strain is either in elastic or in the inelastic region.

CHAPTER II

REVIEW OF LITERATURE

The web in a web line is subjected to tension in MD, but there is no evidence of CMD forces that produce CMD compressive stresses. However for troughs to occur there must be compressive stresses acting in a lateral CMD direction. The transverse cross section of a troughed free span of thin web is similar to a buckled thin plate. Hence analysis of troughed webs can be done similar to the buckling analysis of a rectangular plate which is subjected to loads in both X and Y directions. Timoshenko and Gere [1] have analyzed the buckling of a rectangular plate, subjected to loads in both the directions.

The differential equation for the deflection surface (w) in case of an isotropic plate, under the action of membrane forces is:

$$\frac{\partial^4 w}{\partial x^4} + 2\frac{\partial^4 w}{\partial x^2 \partial y^2} + \frac{\partial^4 w}{\partial y^4} = \frac{1}{D}\left(N_x \frac{\partial^2 w}{\partial x^2} + N_y \frac{\partial^2 w}{\partial y^2} + 2N_{xy}\frac{\partial^2 w}{\partial x \partial y} \right) \quad \{1\}$$

Where N_x, N_y, and N_{xy} are the membrane forces which may serve to increase or decrease the out-of-plane deformations.

In the case of a web in a web line where there are no shear stresses acting the deflection equation can be rewritten as

$$D\frac{\partial^4 w}{\partial x^4} + 2D\frac{\partial^4 w}{\partial^4 x^2 \partial y^2} + D\frac{\partial^4 w}{\partial y^4} - \sigma_x t\frac{\partial^2 w}{\partial x^2} - \sigma_y t\frac{\partial^2 w}{\partial y^2} = 0 \qquad \{2\}$$

Where σ_x and σ_y are the membrane stresses and t is the web thickness and $D = \frac{Et^3}{12(1-\nu^2)}$

Good and Biesel[2] has taken this further and derived an expression for the minimum CMD compressive stress needed to buckle the web, known as the critical buckling stress. For an isotropic web of width ‘b’ that spans the distance ‘a’ between two rollers the governing differential that of equation {1}.

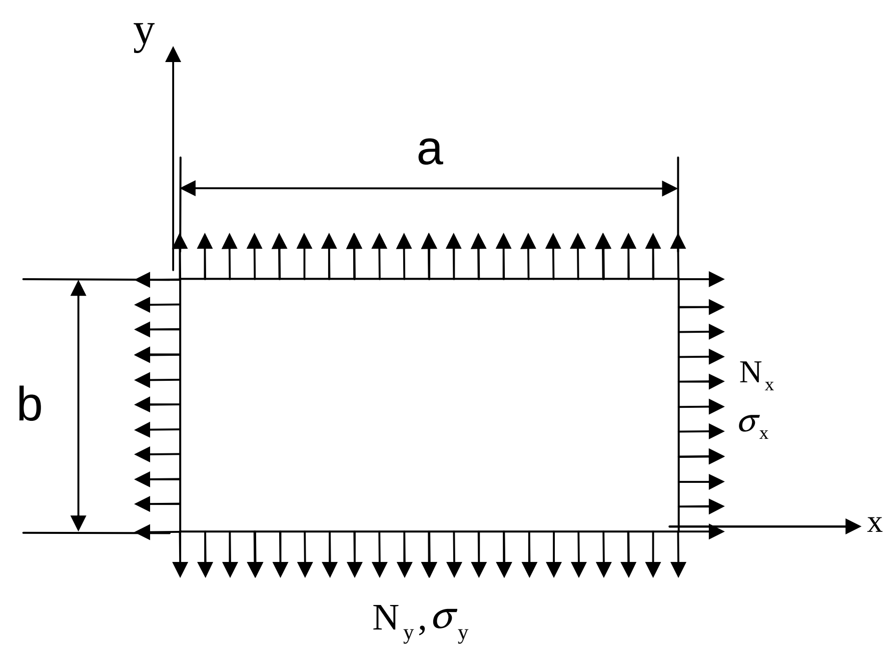

Figure 2.1-Isotropic Span of Web

A solution is sought for the out-of-plane deformation ‘w’ of the form:

$$w = A_{mn} Sin\left(\frac{m\pi x}{a}\right) Sin\left(\frac{n\pi y}{b}\right) \qquad \{3\}$$

where m and n are the half wave numbers in the x and y directions, respectively and A_{mn} is the maximum amplitude of out-of-plane deformation for a given buckled shape. By choosing the displacement of the form {2}, the out of plane deformation is forced to vanish at all four boundaries of the web span when m and n are positive integers. This condition appears to be appropriate when web is in contact with rollers but no constraints exist on the free web boundaries (y=0, b). During the experimental observation of troughs, the out-of-plane deformations near these free edges were minute compared to the out-of-plane deformations associated with the troughs. This behavior could be due to the fact that, compressive CMD stresses do not exist at the free boundaries. The combination of the absence of troughs at edges and that web tension acts to restrict the out-of-plane deformation ‘w’ supports the assignment of the simple support boundary condition to these boundaries (y=0,b). The tension in the web restricts the half wave number in x direction (m) to be unity. Substituting the expression {3} in to expression {2} and solving for σ_y, a relationship for buckling stress is produced of the form:

$$\sigma_{ycr} = -\frac{(b^2 + a^2 n^2)^2 \sigma_e + b^4 \sigma_x}{a^2 b^2 n^2} \qquad \{4\}$$

Where $\sigma_e = \frac{\pi^2 D}{a^2 h}$

Observing expression {4} it can be determined that critical buckling stress σ_{ycr} is a function of half wave number (n) in y direction and tensile stress σ_x in the x direction.

With the increase in magnitude of tensile stress and half wave number (n) in y direction, stability of the web increases. To determine the correct value of n, for a given tension requires consideration of minimum energy. Assuming n as being continuous for the moment, the energy can be minimized by taking derivative of {4} with respect to n, equating the result to zero, solving for n and substituting the result back into the {4}. The resultant expression is

$$\sigma_{ycr} = -2\left(\sigma_e + \sqrt{\sigma_e^2 + \sigma_e \sigma_x}\right) \qquad \{5\}$$

From the expressions {4} and {5} it can be proved that very little (σ_y) CMD compressive stress may induce instability in thin webs. If we select a=30”, E=600,000 psi, ν=0.3, t=.001” , and σ_x=1000 psi we will find that mere -1.55 psi σ_y stress will induce troughs in the web.

E. Cerda and L. Mahadevan [3] discuss about the wrinkling (they refer to trough as wrinkles) in an elastic sheet under tension. The authors developed scaling laws for amplitude and wavelength of trough, and assert these scaling laws are applicable to both isotropic and anisotropic sheets that have been stretched either in the elastic or into the inelastic range. All the authors’ developments consider isotropic materials stretched in the elastic range. Extensions to anisotropic materials or to sheets stretched to the inelastic range are not shown. They state that, when a thin elastic isotropic sheet of thickness ’t’, width ‘W’ and length ‘L’ (where L>W>>t), composed of a material with Poisson’s ratio ‘υ’ and young’s modulus ‘E’ is subjected to longitudinal strain ‘γ’, the sheet remains flat until the applied strain do not exceeds the level strain γ_c called the critical stretching strain. Stretching the sheet further ($\gamma > \gamma_{c)}$ causes the sheet to buckle and form troughs.

In Cerda and Mahadevan’s case the troughs occur due to clamped boundaries. They do not allow the sheet to contract laterally at the clamps which results in a biaxial stress state at the clamps. The CMD stress is tensile near the clamps and compressive slightly further from it. When sheet is stretched beyond the strain γ_c, σ_y becomes less than σ_{ycr}, and the web buckles.

The Authors developed the expressions for wavelength and amplitude by minimizing the total energy. The total energy of a stretched sheet is U = U_B + U_S , where U_B is the bending energy of the sheet and U_S is the energy due to stretching of the sheet, subject to any geometric constraints.

The expression for strain energy in bending for the web stretched in-between two clamps is obtained by simplifying the total strain energy in bending given by Timeshenko [1]

$$\frac{D}{2}\iint\left\{\left(\frac{\partial^2 w}{\partial x^2}+\frac{\partial^2 w}{\partial y^2}\right)^2-2(1-\upsilon)\left[\frac{\partial^2 w}{\partial x^2}\frac{\partial^2 w}{\partial y^2}-\left(\frac{\partial^2 w}{\partial x\partial y}\right)^2\right]\right\}dxdy \qquad \{6\}$$

In the above expression the Authors assume the term $\left(\frac{\partial^2 w}{\partial x^2}\right)$ to be negligible; however they do not give the reason for their assumption. The out-of-plane deformation of a buckled web can be assumed to be of the form $w = ASin\left(\frac{\pi x}{L}\right)Sin\left(\frac{n\pi y}{b}\right)$ where A is the amplitude and λ = n/2b is the wavelength of the troughs. Substituting the out of plane deformation in the expression {6} and solving gives the expression for bending energy.

$$U_B = Et^3\left(A/\lambda^2\right)^2 LW \qquad \{7\}$$

The expression for stretching energy for a web stretched in-between the two clamps is obtained by simplifying the stretching energy given by Timoshenko [1]

$$\frac{1}{2}\iint\left[N_x\left(\frac{\partial w}{\partial x}\right)^2+N_y\left(\frac{\partial w}{\partial y}\right)^2+2N_{xy}\frac{\partial w}{\partial x}\frac{\partial w}{\partial y}\right]dxdy \qquad \{8\}$$

Authors assume $N_y\left(\frac{\partial w}{\partial y}\right)^2$ to be negligible: however they do not provide a reason for their assumption, and solving the expression substituting the out of plane deformation of the above mentioned form, gives the expression for stretching energy as

$$U_s \approx Et\gamma \left(A \Big/ L^2 \right)^2 LW \qquad \{9\}$$

The Authors use a geometric constraint that they call "Geometric Transverse Inextensibility". Although not stated their constraint is a simplification of the large strain expression:

$$\varepsilon_{yy} = \frac{\partial v}{\partial y} + \frac{1}{2}\left[\left(\frac{\partial u}{\partial x} \right)^2 + \left(\frac{\partial v}{\partial y} \right)^2 + \left(\frac{\partial w}{\partial y} \right)^2 \right] \qquad \{10\}$$

The strain ε_{yy} is assumed to be $-\upsilon\varepsilon_{xx}$ which is equal to $-\upsilon\gamma$ in the Authors variables. u,v, and w are the deformation in x, y, and z dimensions respectively. Inextensibility would imply that strain due to in-plane deformation v would be negligible. Also the deformation in the x direction (u) would be nearly constant for a given x location thus the $\frac{\partial u}{\partial y} \Rightarrow 0$.

This leaves us with:

$$\varepsilon_{yy} = -\upsilon\gamma \approx \frac{1}{2}\left(\frac{\partial w}{\partial y} \right)^2 \qquad \{11\}$$

After substitution of w and elimination of constants in the expression {11} leads us to the Authors scaling law:

$$\left(A \Big/ \lambda \right)^2 \approx \nu\gamma \qquad \{12\}$$

Substituting expression {7} in expression {7} and {9}, total energy U can be expressed as

$$U \approx \left(Et^3 \Big/ \lambda^2 + Et\gamma\lambda^2 \Big/ L^2 \right) \nu\gamma LW \qquad \{13\}$$

Minimizing U with respect to λ gives a scaling law for the wavelength

$$\lambda \approx {(tL)^{1/2}}/{\gamma^{1/4}} \qquad \{14\}$$

Substituting the {14} into the transverse inextensibility expression {11} gives a scaling law for amplitude

$$A \approx (\nu t L)^{1/2} \gamma^{1/4} \qquad \{15\}$$

E.Cerda and L.Mahadevan [4] deduced exact expressions with the pre-factors for amplitude and wavelength of troughs formed on thin stretched sheet.

To determine the criterion for selection of the wavelength and amplitude of wrinkles, change in energies of bending and stretching must be accounted. Geometric constraints are imposed using Lagrange multipliers (L). Let the out-of- plane displacement of the initially flat sheet of area W.L be ζ(x,y). $x \in (0, l)$ as the coordinate along the sheet measured from one end and $y \in (0, W)$, (W<<l) as the coordinate perpendicular to it measured from its central axis. Then the total energy function can be written as

$$U = U_B + U_s - L \qquad \{16\}$$

The bending energy U_B due to the deformation which is predominantly in the y direction is given by expression $\frac{1}{2}\int_A B(\partial_y{}^2\zeta)^2\, dA$, where B is bending stiffness or flexural rigidity of the sheet, given by $B = \frac{Et^3}{[12(1-\nu^2)]}$ and U_s is the stretching energy in the presence of a tension T(x) along x direction. The sheet satisfies the condition of transverse inextensibility as it wrinkles under the action of a small compressive stress.

$$\int_0^b \left[\frac{1}{2}\left(\partial_y \zeta\right)^2 - \frac{\Delta(x)}{W} \right] dy = 0 \qquad \{17\}$$

where Δ(x) ~ υγW is the imposed compressive transverse displacement.

Hence the term L in the expression {16} which accounts for the geometric constraints can be expressed as

$$\int_A b(x) \left[\left(\partial_y \zeta\right)^2 - \frac{\Delta(x)}{W} \right] dA \qquad \{18\}$$

where b(x) is the Lagrange multiplier and Δ(x) is the imposed compressive transverse displacement. The Euler-Lagrange equation obtained from the condition of a vanishing first variation of {16}, $\frac{\delta U}{\delta \zeta} = 0$ yields

$$B\partial_y^4 \zeta - T(x)\partial_x^2 \zeta + b(x)\partial_y^2 \zeta = 0 \qquad \{19\}$$

For a stretched sheet T(x) is constant, and Δ(x) ~ υγW is constant far from the boundaries so that b(x) is constant. Away from the free edges in y direction the wrinkling pattern is periodic so that ζ(x,y) = ζ(x,y+2π/k_n), where k_n =2πn/W, and n is the number of wrinkles. At the clamped boundaries ζ(0,y) = ζ(l,y) = 0. Substituting a periodic solution of the form $\zeta = \sum_n e^{ik_n y} X_n(x)$ into the expression {19} yields a Sturm-Liouville-like problem

$$\frac{d^2 X_n}{dx^2} + \omega_n^2 X_n = 0, \qquad X_n(0) = X_n(l) = 0 \qquad \{20\}$$

Where $\omega_n^2 = (bk_n^2 - Bk_n^4)/T$. b is the compressive stress and can be determined from the nonlinear geometric constraint {18}. The solution to equation {20} when b is constant is

$$X_n = A_n Sin \omega_n x \qquad \omega_n = m\pi/l$$

For bending energy to be minimum there should be only on half sine wave along the length, therefore m=1 hence $\omega_n = \pi/L$ so that $b_n(k_n) = \frac{\pi^2 T}{l^2 k_n^2} + Bk_n^2$ and the displacement function ζ is

$$\zeta = A_n \mathrm{Cos}(k_n y + \phi_n)\mathrm{Sin}\, {}^{\pi x}\!/_{l} \qquad \{21\}$$

Plugging the obtained displacement function ζ into the geometric constraint expression {18} yields

$$\frac{A_n^2 k_n^2 W}{8} = \Delta \qquad \{22\}$$

After substituting ζ in the expressions for bending energy U_B and stretching energy $U_{s,}$ the total energy can be written as

$$U = Bk_n^2 \Delta l + \frac{\pi^2 T \Delta}{k_n^2 l} \qquad \{23\}$$

Minimizing the total energy {23} and using the geometric constraint {18} wavelength $\lambda=2\pi/k$ and amplitude A are obtained and are given as

$$\lambda = 2\sqrt{\pi}\left(\frac{B}{T}\right)^{1/4} l^{1/2} \qquad\qquad A = \frac{\sqrt{2}}{\pi}\left(\frac{\Delta}{W}\right)^{1/2}\lambda$$

Substituting the value of flexural rigidity B and tension T for a stretched sheet yields Wavelength to be

$$\lambda = \frac{(2\pi l t)^{\frac{1}{2}}}{\left[3.\gamma.(1-\nu^2)\right]^{\frac{1}{4}}} \qquad \{24\}$$

and Amplitude

$$A = (\nu t l)^{\frac{1}{2}} \left[16\gamma \frac{1}{3\pi^2 (1-\nu^2)} \right]^{\frac{1}{4}} \qquad \{25\}$$

To verify these expressions of wavelength E. Cerda and Mahadevan [4] had stretched different lengths of polyethylene of thickness ~ 0.01cm and width of 12cm at the strain levels of $\gamma \in [0.01, 0.2]$. The polyethylene sheet was clamped between the two aluminum plates to enforce the boundary conditions. The sheet was first taped to one of the aluminum plate using an adhesive tape so that slippage would not occur. A plot showing $1/\gamma^{1/4}$ on x axis and $\lambda/(tL)^{1/2}$ on y axes is plotted with experimental values and theoretical values, a quantitative agreement is obtained.

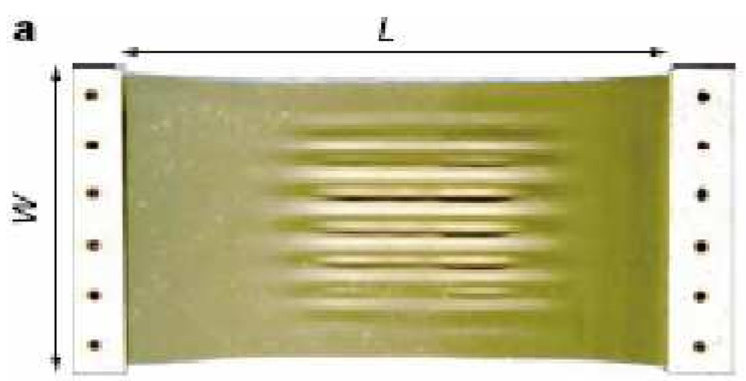

Figure 2.2- Photograph of the sheet depicting the troughs

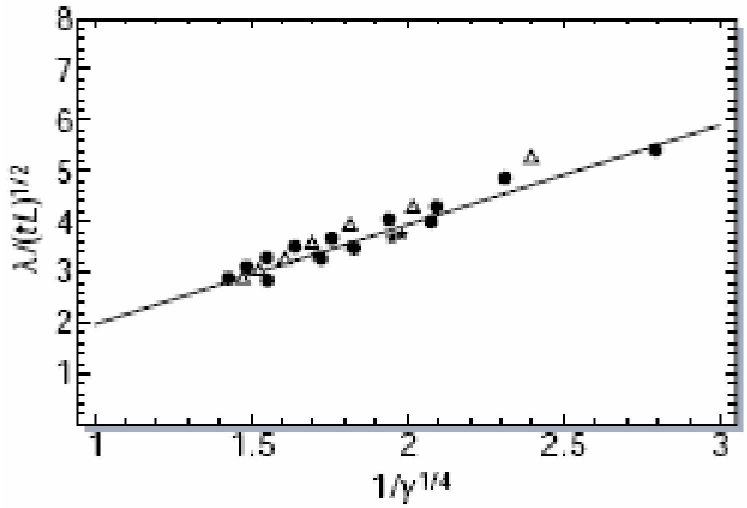

Figure 2.3-Dimensionless wavelength Vs Strain

The expression obtained for amplitude and wavelength by using a double Sine function for the out-of-plane displacement which Timoshenko and Gere yielded the same expressions for amplitude and wavelength. Considering the expression {3} for the CMD compressive stress, and minimizing it with respect to n and solving for n gives an expression for n

$$n = \frac{b}{L}\sqrt[4]{\frac{\sigma_e + \sigma_x}{\sigma_e}} \qquad \{26\}$$

The wavelength can be expressed in terms of λ and width b. Consider there are n number of half sine waves distributed uniformly throughout the width of the web. The distance between the two same points on alternate half sine waves is the wavelength. Hence it can be expressed as $\lambda = \frac{n}{2b}$.

Substituting the expression for σ_e, expressing σ_x in terms of strain γ and Young's modulus E and n=2bλ in expression {26} yields

$$\lambda = \sqrt{2\pi L t}\sqrt[4]{\frac{1}{3(1-\nu^2)\gamma}}$$

Similarly expression for amplitude can be obtained by considering the displacement function for out of plane displacement to be

$$\zeta = ASin\left(\frac{\pi x}{L}\right)Sin\left(\frac{n\pi y}{b}\right) \qquad \{27\}$$

Substituting the expression {27} into the condition of transverse inextensibility {18} and integrating it over x (0, L) and y (0, b) and using the expression for wavelength yields

$$A = \sqrt{\nu Lt}\sqrt{\frac{16}{3\pi^2(1-\nu^2)}\gamma^{1/4}}$$

Research Objective:

Cerda and Mahadevan have developed a condition of "Transverse Inextensibility" to define the amplitude of troughs and the wavelength of troughs. The expression for wavelength is equivalent to that which can be derived from Timoshenko expressions. The expression for amplitude is novel. Cerda et al claim these expressions applicable to isotropic and anisotropic materials in the elastic and inelastic domains of strain. The Authors lend some proof in this context by wavelength measurements of troughs in polyethylene web over a large range of strain. They provide no proof of their scaling laws for amplitude and how they are impacted by inelastic strain.

The objective of this research is to determine if Cerda and Mahadevan's claims are credible or if not under what conditions they are credible.

CHAPTER III

EXPERIMENTAL SETUP AND MATERIAL CHARECTERIZATION

The equipment required for the Research was provided by the Web Handling Research Center at Oklahoma State University. To conduct the experiments we needed a universal testing machine, a sensor capable of capturing the troughs profile and load cell to determine the load, and user interface to note the readings.

Experimental Setup for Profile of Trough:

The experimental setup consisted of equipment capable of holding, stretching the web and measuring the wavelength and amplitude of troughs. An Instron Universal Testing Machine was used to stretch the web; the maximum stroke of the machine was around 4 inches. The web was supported between the hydraulic ram and the load frame of the Instron using two aluminum clamps. To have a good adherence, rough rubber strips were used in-between aluminum clamps and web, the rubber strips were adhered to the aluminum clamps using a strong adhesive. As the web was stretched, in-between the clamps, a tensile load developed. An external S-type load cell was calibrated to measure the low load levels applied to the web, as it was stretched at different strain levels. At low strain levels, these troughs appear whose average amplitude is of the order of 10^{-2} inches. A Laser sensor was used to capture the out-of-plane deformation associated with these troughs. A Keyence model LC-2100 laser sensor was used. The sensor is capable of resolving a change in distance of 1/1000th of an inch, thus the out-of-plane deformation of the troughs can be captured using this sensor. The sensor ejects a laser beam of light, this beam after reaching the object gets reflected and return to the sensor. The distance between the object and sensor is measured using the time taken by reflected beam to reach the sensor. Using this sensor we can measure the out-of-plane deformation of a point on the web. To get the profile of the trough across the width of the web, the Keyence sensor is forced to move in the cross machine direction on a linear bearing. The position of the Keyence sensor is measured using a Yo-Yo pot. A Yo-Yo pot transduces linear motion to a change in resistance. The variable resistance becomes a part of a ballast DC circuit where the voltage drop across the variable resistance is calibrated with respect to the linear motion that requires measurement. A data acquisition system consisting of a National Instruments SCB-68 A/O board, a computer, and a Lab-View software program were used to simultaneously record the output from the Keyence 2100 laser sensor and the Yo-Yo pot. In this way the trough amplitudes as a function of CMD location was recorded.

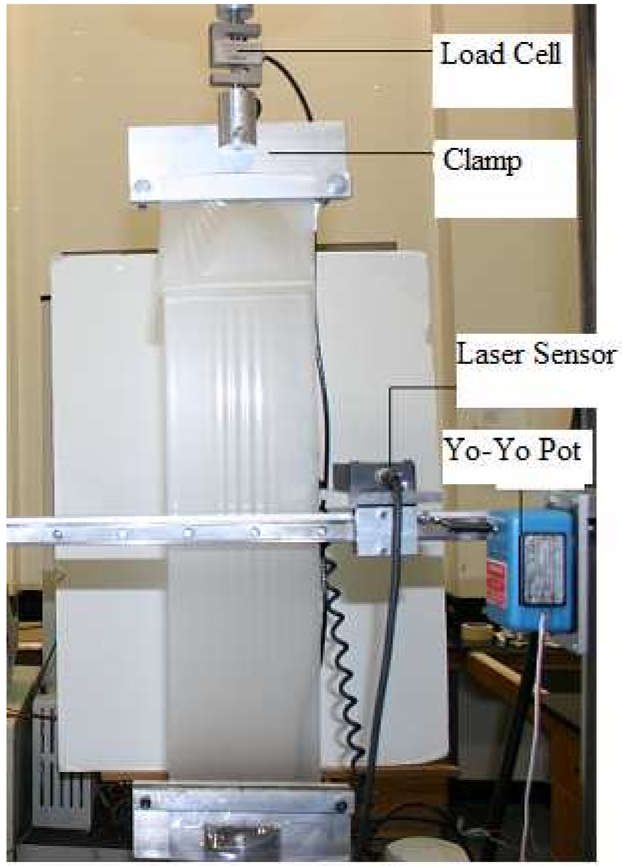

Figure3.1-Experiment Setup

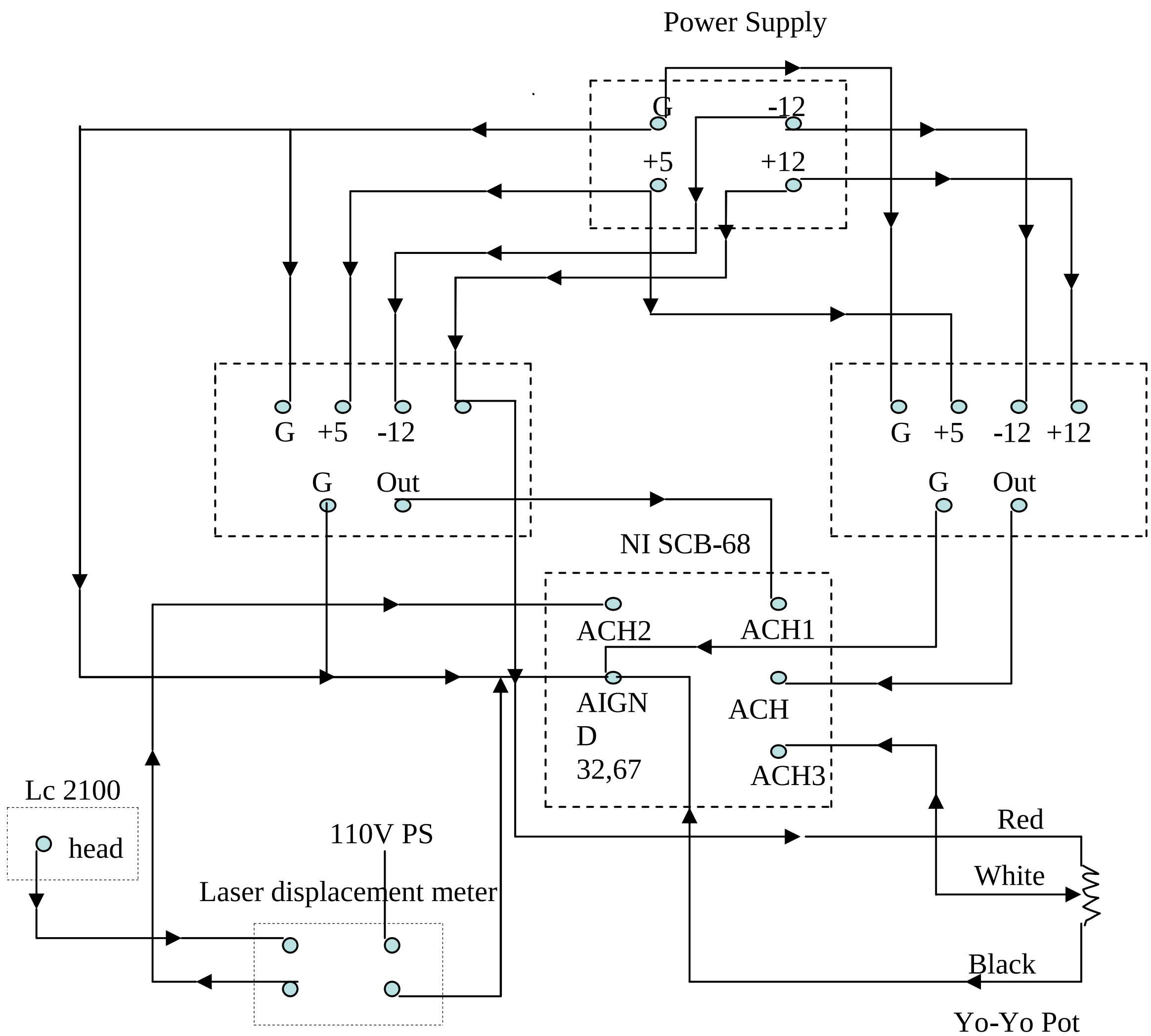

Figure 3.2-Schematic Circuit Diagram

Material Characterization:

The expression for wavelength and amplitude given by Cerda[] involve material properties such as Young's Modulus and Poisson's ratio. Therefore to get correct values of amplitude and wavelength it is required to have good knowledge of material properties. To prove or disprove Cerda's claim we must know how these web properties change as the strain level enter the inelastic range.

There were two tests conducted to determine the Young's Modulus, the Tangent Modulus and Poisson's ratio of a low density polyethylene web material, similar to that used by Cerda.

Modulus Testing:

The stretch test was performed on a 50' long and 10'' wide test specimen of LDPE. A load transducer was attached to the test specimen, and was elongated to a length of approximately 65'. For every one unit change in the load applied recorded from the transducer, the associated change in length or elongation of the specimen was noted. Strain and stress can be calculated using the elongation and load respectively. Stress and strain plotted on Y and X axes respectively gives stress-strain curve. The slope of stress and strain curve in proportional range of stress and strain is the Young's Modulus.

The tangent modulus at inelastic strain levels can be determined using the same test data.

Figure 3.3- 60’’ web stretched on the floor to run the stretch test

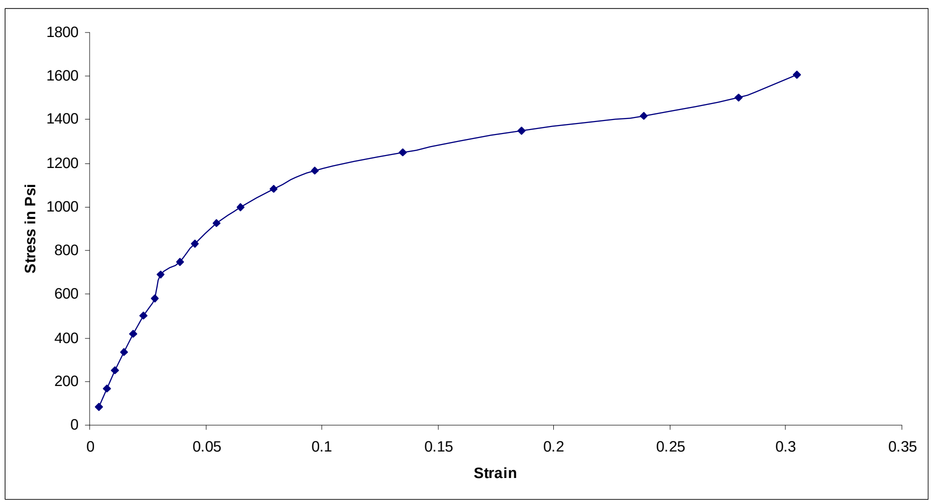

Figure 3.4-Stress-Strain Curve for a Polyethylene web material

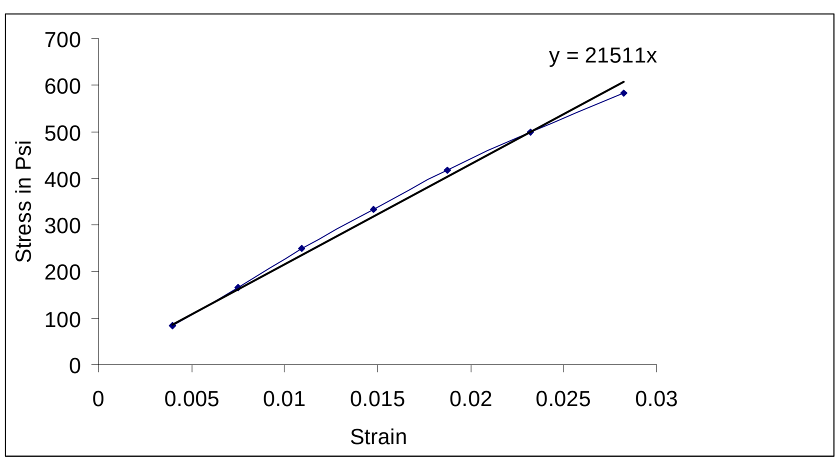

Figure 3.5-Elastic Strain Vs Stress Showing Young’s Modulus (E) =21511

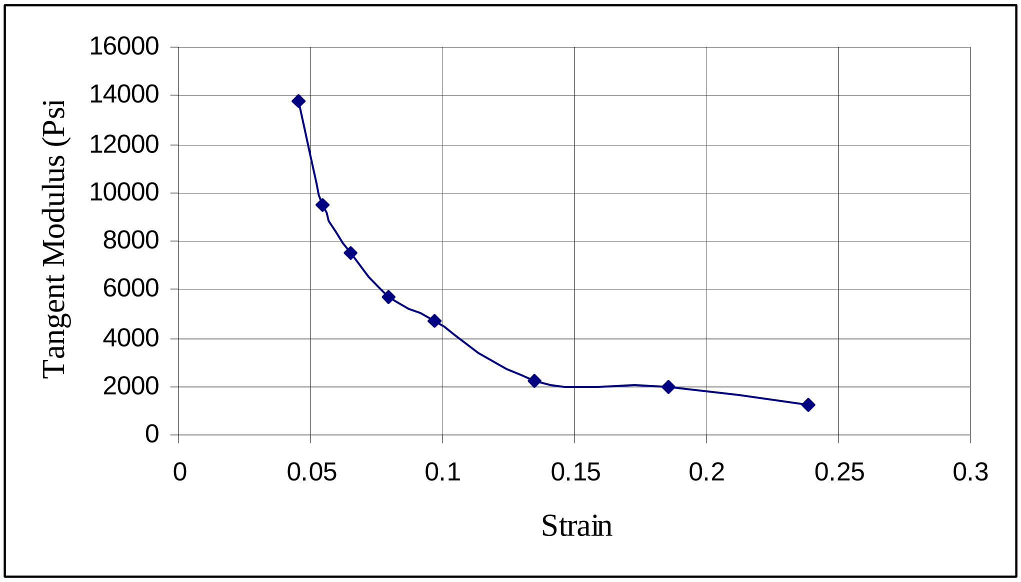

Figure 3.6-Tangent Modulus along the strain

Measurement of Poisson's Ratio:

The Poisson's ratio varies from 0.3 to 0.5 for the polyethylene material. According to the literature it seems that the Poisson's ratio abruptly changes from 0.3 to 0.5 as soon as the material reaches it plasticity. We were interested in determining the Poisson's ratio at each strain levels over the domain in strain where Young's modulus and the Tangent modulus were measured. Poisson's ratio is defined as the minus ratio of lateral strain and longitudinal strain. The measuring of longitudinal strain in the web was achieved by tracking the movement of ram on the Instron machine. The change in the ram position is the measure of change in the length of the web. Since the width of the web was only 6'' inches it was hard to determine the change in width. Apart from this, the occurring of troughs would hinder the measurement process.

A photographic method was used to determine Poisons ratio. The web was marked with two pair of dots each apart by 1’’, one along MD and one along CMD, between the two web clamps on the Instron machine and a photograph was captured using a high resolution manual lens camera at various strain levels. A flat field macro lens was selected as its focus remains constant through the field of view, as for a typical lens focus varies, which would induce error in the Poisson’s ratio measurement. The distance between the dots was measured using drawing tools within Microsoft Paint.

Since the distance between two pair of dots was known in terms of the number of pixels, the scaling factors for determining the actual distance from the number of pixels between the two points in the photographs could be defined as the ratio of the actual distance between the points and the number of pixels. Photographs at each strain level were captured and the change in distance between the two pair of dots in CMD and MD was measured. The ratio of change in the distances and original length and width would give the respective strains. Minus the ratio of the lateral strain and longitudinal strain would give us Poisson’s ratio.

After the experiments were performed the Poisson’s ratio determined was greater than 0.5 even when the material was in elastic range, which indicated that there was an error in the experiment. The reason for getting such values for Poisson’s ratio was due to formation of troughs, even though the dots were marked at a place where the troughs formation just started or the point where the CMD tensile stresses vanished. The trough formation had a prominent effect on measurement of Poisson’s ratio.

Figure 3.7-Photograph of the two pair of dots at a strain of 0.0398

In order to avoid this, a roller was placed such that it will touch the web right at the points where the dots are marked to prevent out-of-plane trough deformations. As the stroke of the Instron machine is 4'' inches the roller cannot be in contact with the web at all the strains. Therefore the roller was mounted such a way that it could be moved by hand in the MD. Care was taken that the friction between the roller and the web will not hinder the lateral movement of the dots. The Poisson's ratio was measured over large range of strain.

The test was conducted twice to check the repeatability and accuracy of the experiment. The Poisson's ratio at different strain levels from both the experiments were plotted on the graph shown below and a curve was fit so that a specific value could be determined for Poisson's ratio at all strain levels, using the expression from the curve fit. The curve fit equation was '$\nu(\gamma) = 80.62\gamma^3 - 31.81\gamma^2 + 4.008\gamma + 0.2994$'. {28}

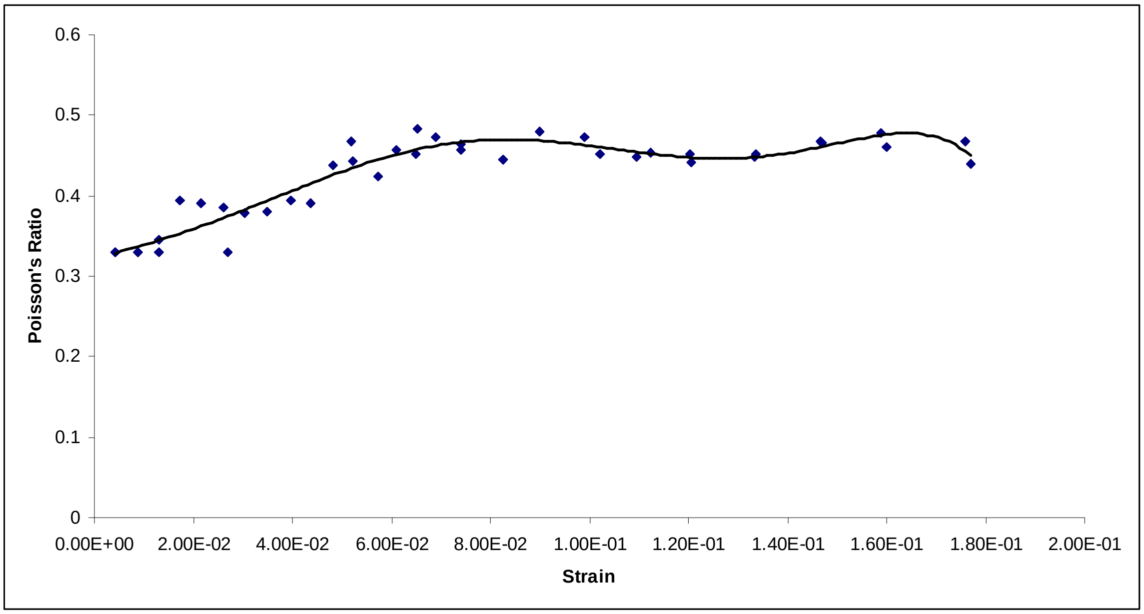

Figure 3.8-Graph of Poisson's ratio VS strain

Strain	Tangent Modulus *ET*	Poisson's ratio
0.045	13745 psi	.422
0.054	9482 psi	.436
0.064	7500 psi	.447
0.079	5674 psi	.457
0.097	4705 psi	.462
0.135	2204 psi	.463

Table 3.1- Tangent Modulus and Poisson's Ratio of LDPE Web

CHAPTER IV

EXPERIMENTS AND MODELLING

Experiment to Determine the Trough Profile:

A 6’’ wide 100 gauge polyethylene web was used in the study. The experiments were conducted on specimens with different aspect ratios (length/width) ranging from 4 to 5 in their undeformed state. A web of fixed length was installed in aluminum clamps. The clamps were setup with high friction surfaces to prevent slippage of the web in the clamp in the MD and CMD directions. Care was exercised such that the two aluminum clamp surfaces lie in the same plane. This was done to prevent bending and torsional loads from influencing the result. Also the web was fixed such that it was perfectly orthogonal to both the clamps. A servo hydraulic material testing system (Instron Model 8502) was used to precisely stretch the web. Two black lines were drawn on the web, where it enters the clamps at beginning of the experiment. If the lines remain straight after the experiment it was an indication that slippage did not occur during the experiment.

The Finite Element Method was used to analyze the internal stresses in the web, fixed at both the ends, but subject to MD tension. CMD tension resulted in at the near vicinity of clamps, and then CMD compressive stresses developed away from the clamps before the stresses died out. These regions of pockets of compressive CMD stresses were located about 10’’ away from the clamps irrespective of the test span length or aspect ratio of test specimen. The results of these analyses were that all test specimens were chosen with lengths exceeding 20” such that CMD compressive stresses and hence instability would occur.

Three sets of experiments were conducted and each set had different specimen length and an aspect ratio. To test the repeatability each specimen length was tested thrice. In the first set of experiments the specimen was chosen to be 24’’ long. This specimen was stretched to a strain level of 0.132. The troughs started appearing at a very low strain level of 0.005. The out-of-plane deformation of the trough was captured using a Keyence (Model 2100) laser sensor. The second and third set of experiments, were conducted on test span lengths of 27’’ and 30’’. The troughs were formed at almost same strain level as formed on 24’’ test specimen.

In order to confirm that these troughs were not formed due to the pocket of compressive stress, a 12’’ test specimen was tested, stretching it to a strain level of 0.254. There were no prominent troughs formed on the web even at highest strain level achieved.

Modeling of Troughs Formation Using ABAQUS:

Finite Element Modeling was used to model the trough formation witnessed in the laboratory. The FEA package ABAQUS Explicit was used to model the laboratory procedure. The web was modeled in a 3D modeling space as single section with shell elements. A structured mesh with quad dominated element shape was used. A ‘S4R’ element which is a 4 node shell element with reduced integration. The clamping of the web at the ends was modeled using the boundary condition. At one end, the web movement was constrained in 6 DOF (U_x, U_y, U_z, R_{xy}, R_{yz} and R_{zx}) and on the other end the movement was constrained in 5 DOF(U_y, U_z, R_{xy}, R_{yz} and R_{zx}) leaving the web free to move in the direction of the applied displacement U_x. To model the stretching of the web displacements were enforced to the U_x DOF. For every strain level an enforced displacement was given as a boundary condition. The displacement was applied in steps using an amplitude-time curve.

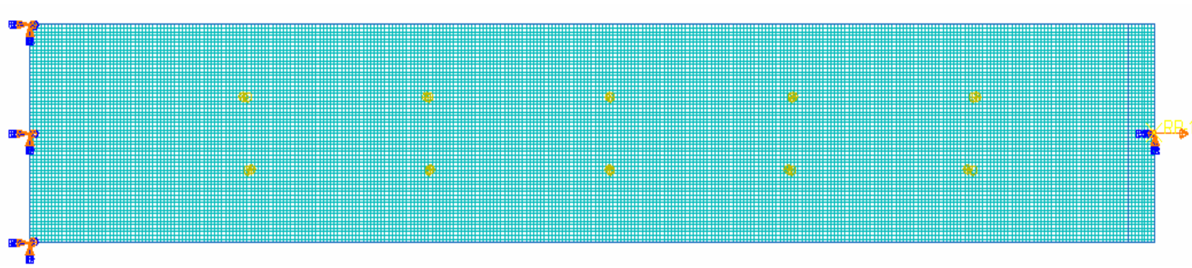

Figure 4.1- Depicting the modeling of the web and positions of ghost force

The global seed of the mesh was chosen to be 0.05”; that is each element has an edge of length 0.05”. The accuracy of the trough wavelength depended on this mesh size. The finer the mesh more provided greater the accuracy of the wavelength, but also increased the run time of the simulation. Thus this mesh size was chosen to optimize the run time of the simulation without jeopardizing the accuracy of the wavelength.

Mathematically instability will not occur when the structure is subjected to tension. Commercial finite elements codes which are in use as of today cannot automatically simulate the behavior of the thin structures buckling in tension. To simulate the buckling behavior of the web in ABAQUS an out-of-plane load must be applied, called ghost force, in order to induce some instability in the structure. In order to minimize the influence of the ghost load on amplitude and wavelength on troughs formed, it was applied in such a way that it vanishes after instability was induced in the structure. In order to accomplish this, a second amplitude-time curve was used to vary the amplitude of the ghost force. Pairs of equally spaced positive and negative concentrated ghost forces were applied to web. The stresses induced due to these forces were negligible when compared to tensile stresses that resulted from stretching of the web. The nonlinear analysis occurred over 10 time solution steps. The enforced displacements which induced the strain desired in the simulation became maximum in time step 2. The ghost load became maximum in the time step 5 and vanishes in the time step 7. The out-of-plane deformations were examined in the time step 8 through 10 to determine if instability had occurred.

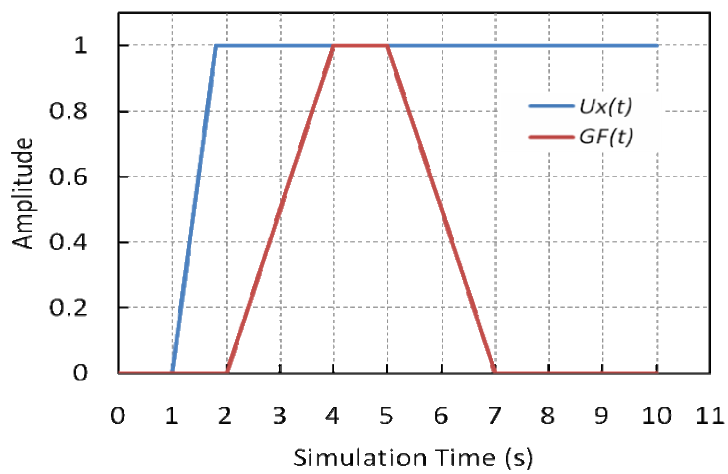

Figure 4.2- Showing the two Amplitude-time curves

The simulations were run at several strain levels for the three different lengths web specimens tested (23", 27" and 30"). After completion of the simulation, the out-of-plane deformation (U_z) were examined and used to calculate the amplitude and wavelength of the troughs formed.

The simulation was run initially using ABAQUS Standard, but the amplitude of the troughs appeared to be dependent on the magnitude of ghost force. Then ABAQUS Explicit was used to run the simulation. The dependency of the amplitude of out-of-plane deformations due to the magnitude of ghost forces in case of ABAQUS Explicit is shown in the figure. Since there is no dependency it is assumed that the amplitudes of the out-of-plane deformations computed are realistic.

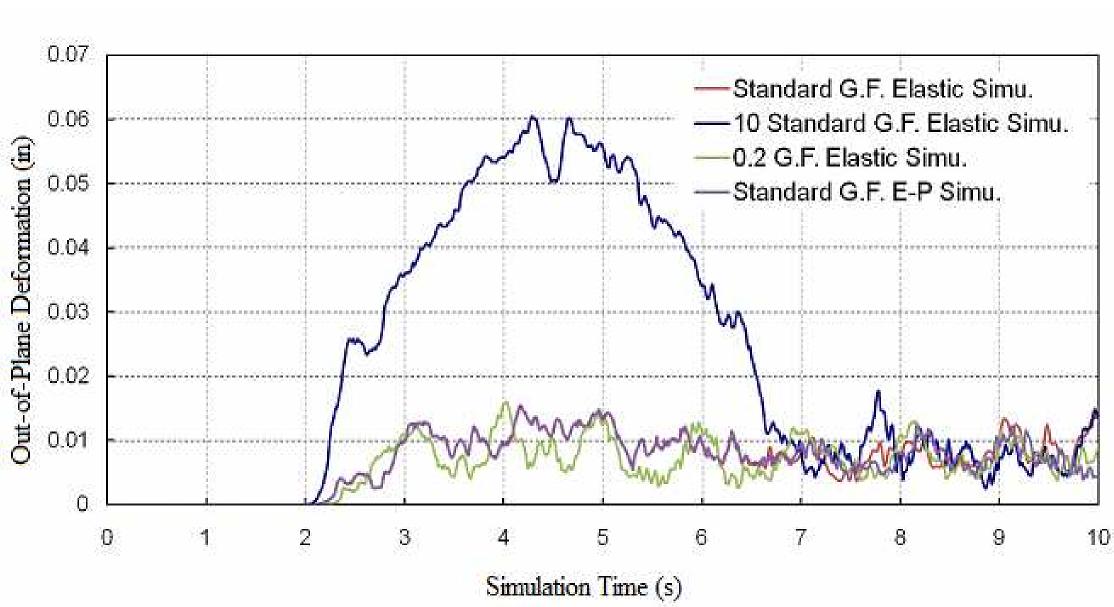

Figure 4.3-Depicting the influence of ghost force on Out-of-plane Deformation with time.

CHAPTER V

RESULTS and COMPARISIONS

Experimental Results:

The out-of-plane deformations for the three test span lengths at different strain levels were obtained. The out-of-plane deformations for a particular strain level of 0.0165 on a 24” long web is shown below. The results for other strain levels and web lengths are shown in the appendix.

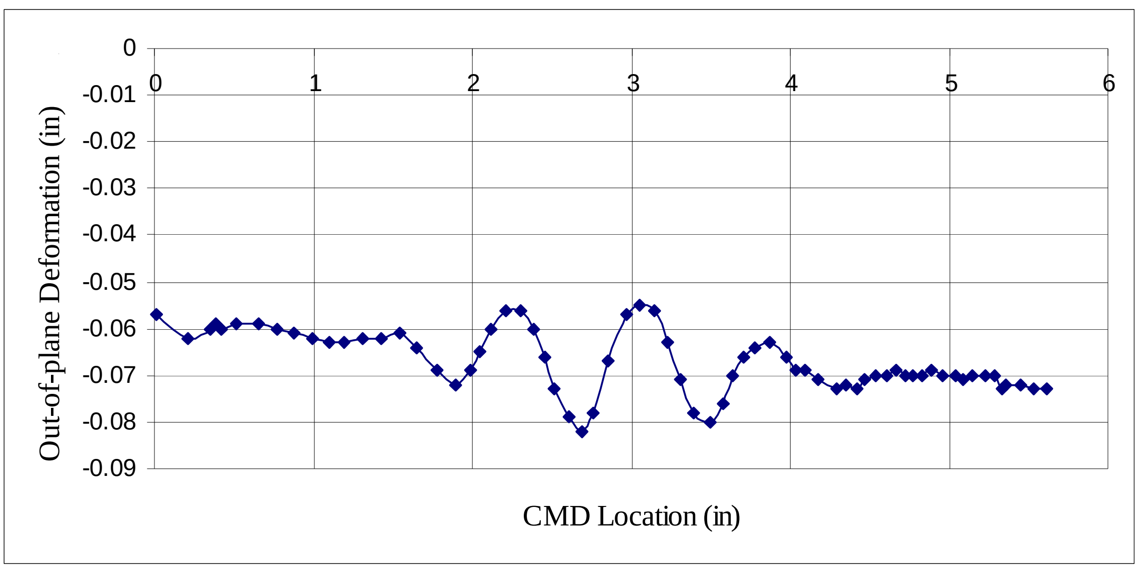

Figure 5.1-Out-of-plane deformation of 24” test specimen at a strain of 0.016

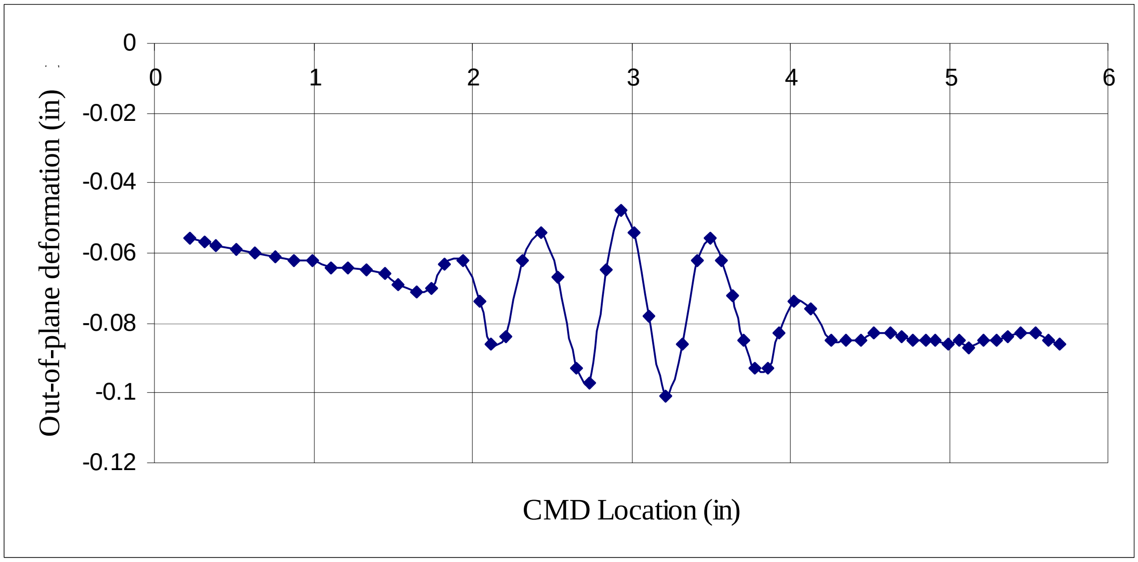

Figure 5.2-Out-of-plane deformation of 24” test specimen at a strain of 0.132

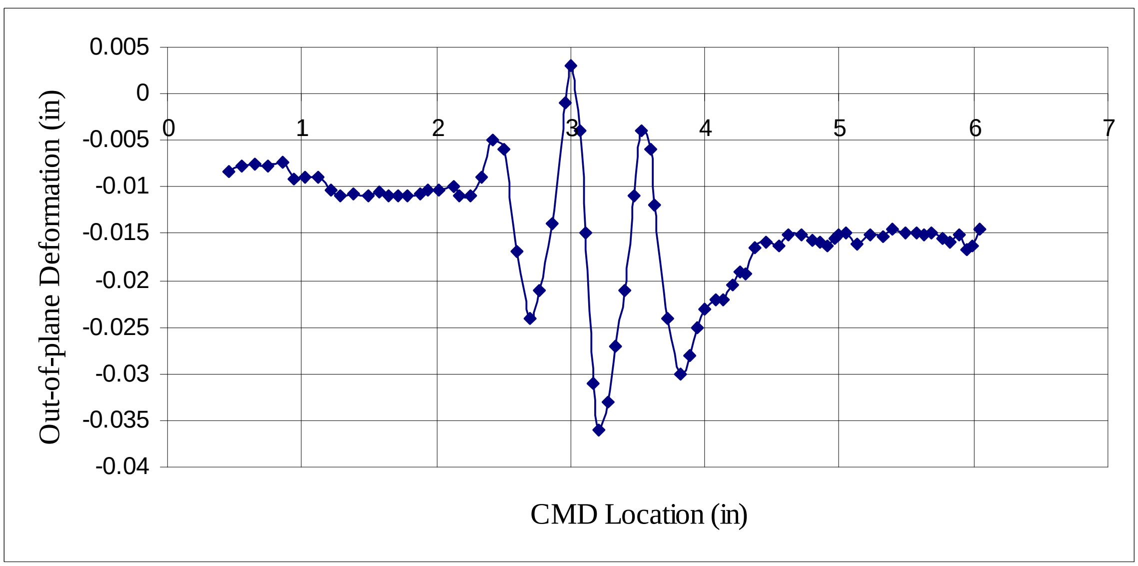

Figure 5.3-Out-of-plane deformation of 27” test specimen at a strain of 0.1296

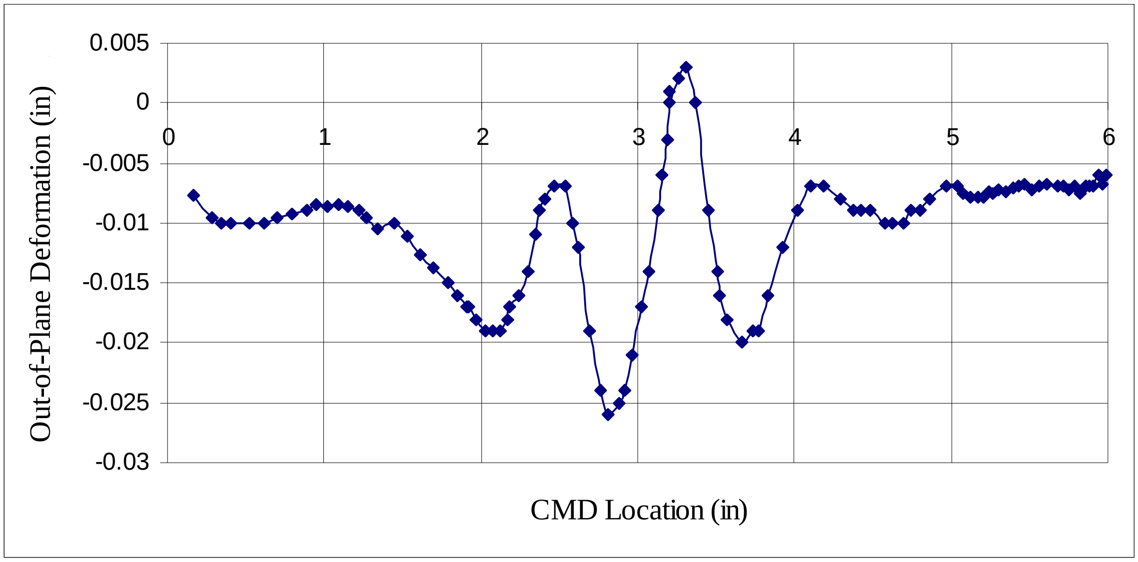

Figure 5.4-Out-of-plane deformation of 30” test specimen at a strain of 0.033

To verify the repeatability of the experiment all the test specimens were tested for three times and the results where compared.

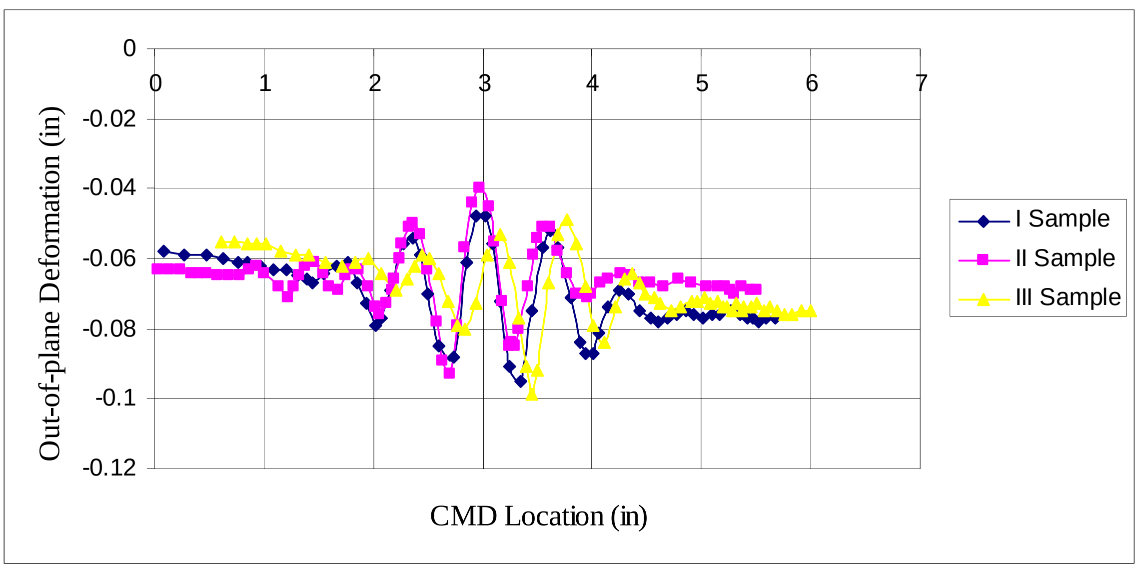

Figure 5.5-Out-of-plane deformations of three 24” test specimens at strain of 0.049

Observing the above out-of-plane deformation graphs, there is a general left to right decrease in the deformation, this could be due to the fact that the line of travel of the keyance sensor may not be perfectly parallel to the web when mounted on to the Instron machine. This may not affect the accuracy of the amplitude as the width of a typical trough is less than one half of an inch and the method of measuring the amplitude of a trough is independent of the positions of other trough. The actual deformation can be obtained by deducing the angle between the web plane and line of travel of the sensor using the linear regions on the either side of the buckled web.

The amplitude and wavelengths from all the three test spans were obtained and the error was calculated.

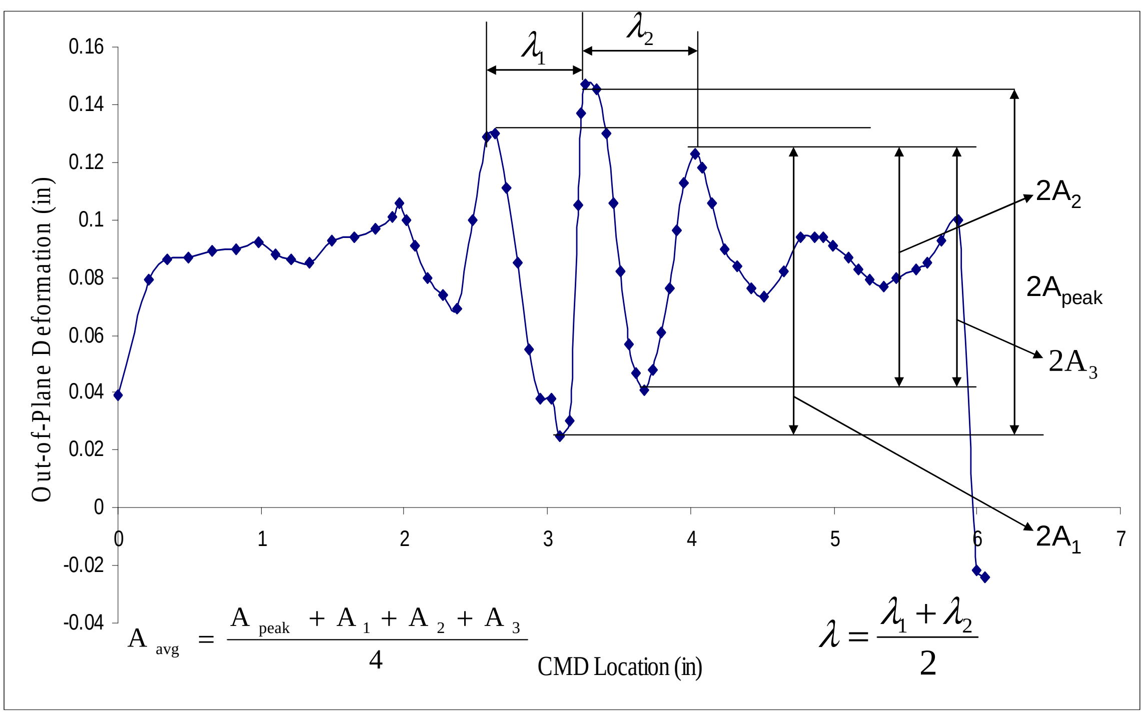

Figure 5.6- Depicting measurement of Amplitude and Wavelength

The table depicts the error in the amplitude and wavelength from three different test specimens of same length.

Amplitudes of 24" Test span at different strain levels (P-P Values)

Strain	I	II	III	Avg (in)	Error(in)
0.0165	0.0222	0.02075	0.02167	0.02154	0.000734
0.033	0.0294	0.028	0.0278	0.0284	0.000872
0.0495	0.0325	0.0331	0.0368	0.034133	0.002329
0.066	0.0376	0.031	0.0391	0.0359	0.004309
0.0825	0.0368	0.0281	0.0347	0.0332	0.00454
0.099	0.04025	0.0268	0.0337	0.033583	0.006726
0.1155	0.03712	0.031	0.0347	0.034273	0.003082
0.132	0.0323	0.031	0.0304	0.031233	0.000971
0.1485	0.0328	0.0295	0.0225	0.028267	0.00526

Table 5.1-Average Amplitude and Error of three different test specimens of 24" long

Amplitudes of 30" Test span at different strain levels (P-P Values)

Strain	I	II	III	Avg (in)	Error(in)
0.0165	0.0164	0.0158	0.018	0.0167	0.0011
0.033	0.0192	0.02	0.021	0.02	0.00090
0.0495	0.0228	0.0208	0.0213	0.0216	0.0010
0.066	0.0234	0.02	0.0236	0.022	0.002
0.0826	0.021	0.017		0.019	0.0028
0.099	0.0213	0.0148		0.0180	0.004
0.1157	0.02	0.0126		0.0163	0.005
0.132	0.019	0.012		0.0155	0.004

Table 5.2-Average Amplitude and Error of three different test specimens of 30" long

24 in Test Specimen

Strain	I	II	III	Average(in)	Error(in)
0.0165	0.744	0.776	0.759	0.759	0.016
0.033	0.67	0.7003	0.7	0.69	0.017
0.0495	0.618	0.639	0.574	0.61	0.033
0.066	0.6005	0.5946	0.543	0.579	0.031
0.0825	0.556	0.581	0.5257	0.554	0.027
0.099	0.56525	0.5685	0.484	0.539	0.047
0.1155	0.55825	0.519	0.517	0.531	0.023
0.132	0.519	0.511	0.489	0.506	0.015
0.1485	0.5485	0.4866	0.4447	0.493	0.052

Table 5.3-Average Wavelength and Error of three different 24 in long test specimen

30 in Test Specimen

Strain	I	II	III	Average(in)	Error(in)
0.0165	0.892	0.964	0.999	0.951	0.0545
0.033	0.822	0.8035	0.8145	0.8133	0.0093
0.0495	0.7265	0.701	0.759	0.728	0.029
0.066	0.6795	0.64625	0.6966	0.674	0.0256
0.0826	0.669	0.673	0.6035	0.648	0.039
0.099	0.623	0.6645	0.553	0.613	0.056
0.1157	0.6105	0.6265	0.559	0.598	0.035
0.132	0.61	0.624	0.5536	0.595	0.037

Table 5.4-Average Wavelength and Error of three different 30 in long test specimens

Simulation Results:

The Simulation was run for all the three test specimens at different strain levels and the amplitude and wavelength were measured from the out-of-plane deformations obtained in the simulation.

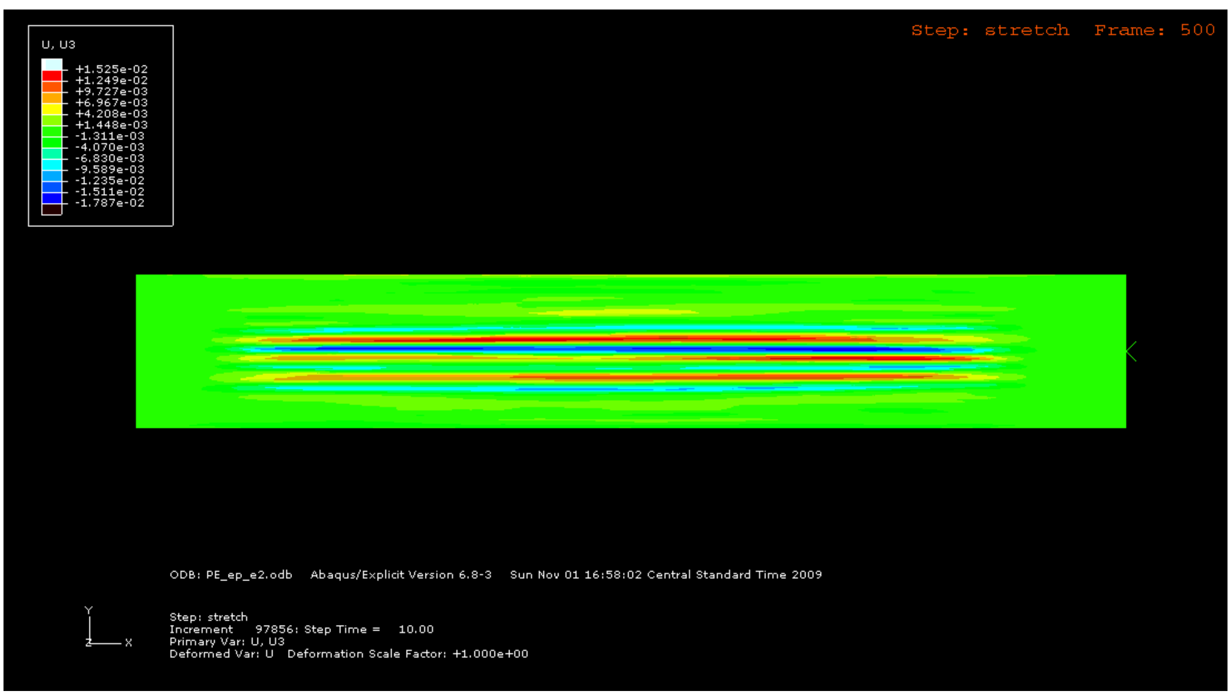

Figure 5.7-The contour plot of out-of-plane deformation of a 24" web at a strain of .0495

The out-of-plane deformation of each node was obtained using a probe value function available in Abaqus, these vales when plotted against the width gives us the trough profile.

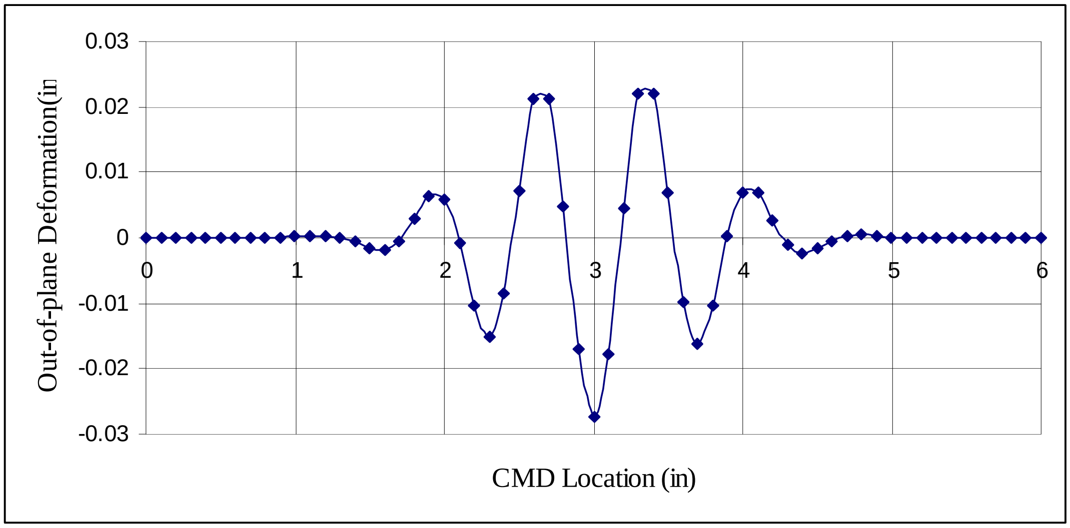

Figure 5.8-Out-of-plane deformation of a 27” web from simulation at strain of .0555

Comparisons:

The values of amplitude and wavelength from experiments and ABAQUS simulation were compared against the closed form solution {24, 25} given by Cerda.

The Poisson’s ratio needed to determine the amplitude and wavelengths of troughs from the closed form solution is obtained from the expression for Poisson’s ratio in-terms of strain $\nu(\gamma) = 80.62\gamma^3 - 31.81\gamma^2 + 4.008\gamma + 0.2994$. The web was 6” wide with a thickness of 0.0012”.

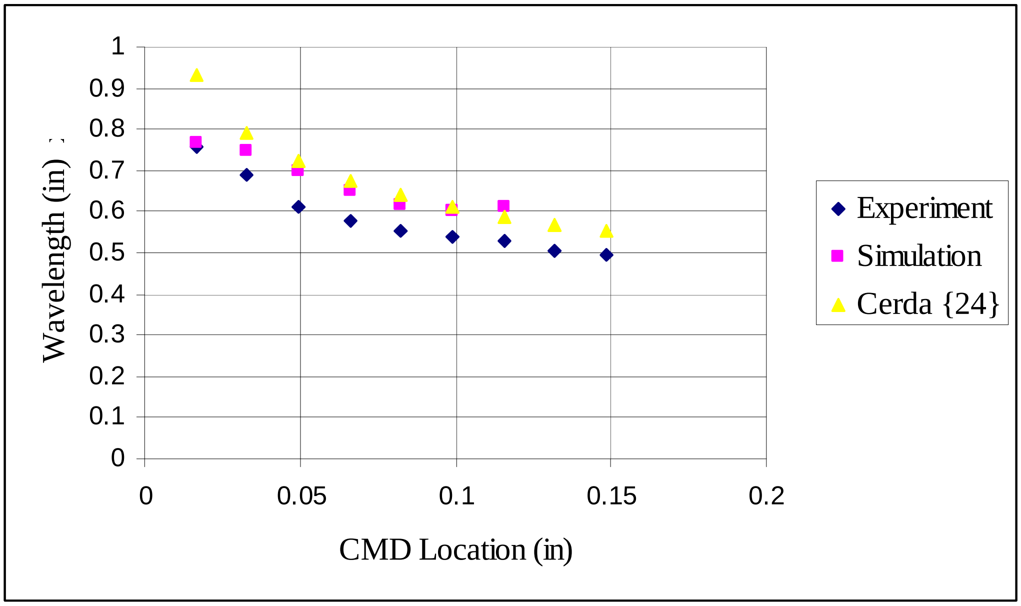

Figure5.9-Wavelengths of the out-of-plane deformation in a 24 in test specimen

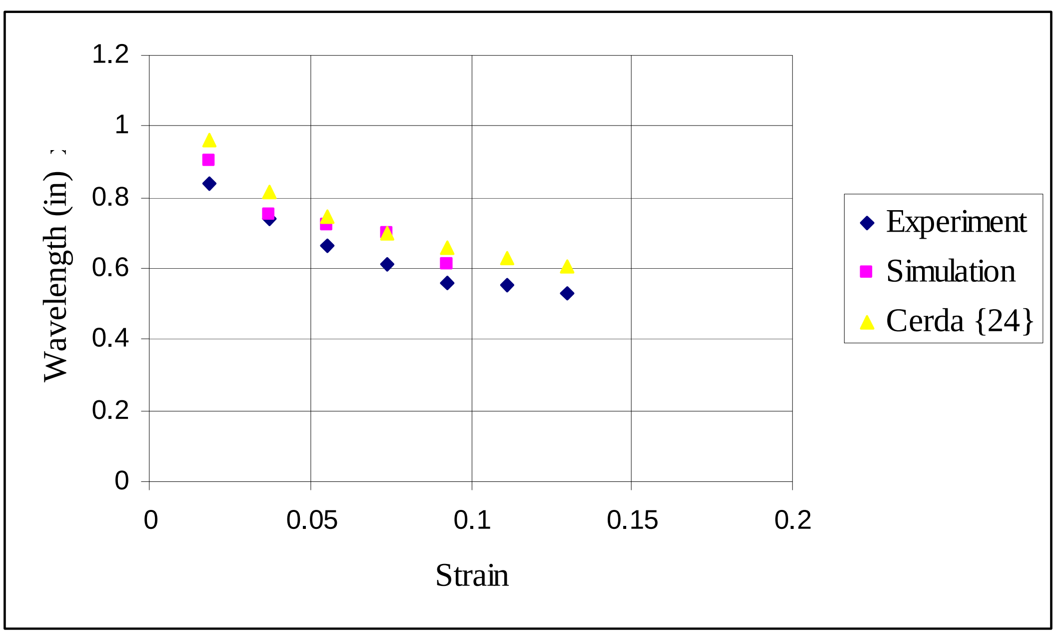

Figure 5.10-Wavelengths of the out-of-plane deformation in a 27 in test specimen

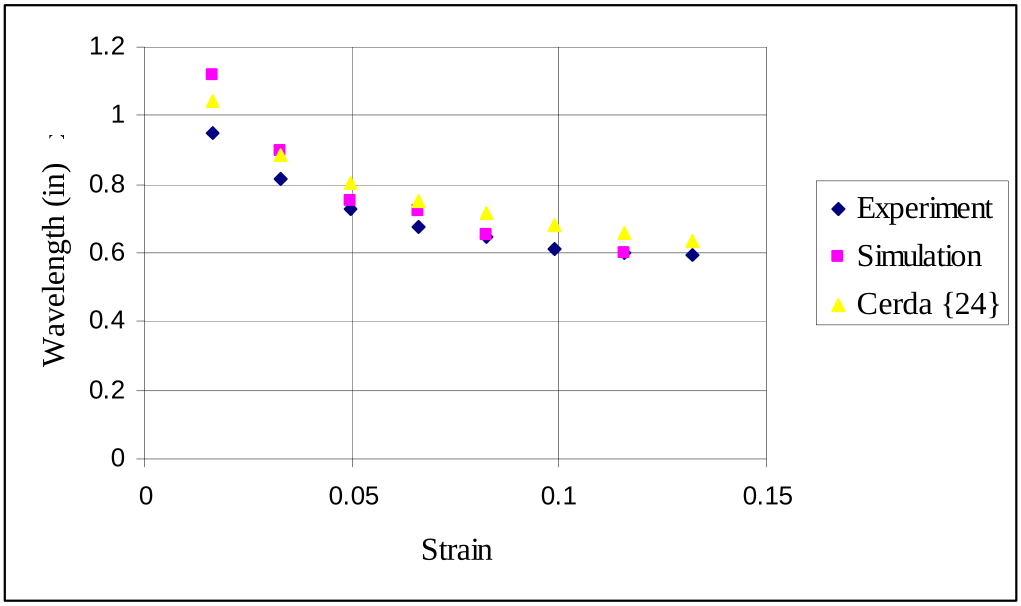

Figure 5.11-Wavelengths of the out-of-plane deformation in a 30 in test specimen

Finally from the figure 4.9, 4.10, 4.11 the results for the wavelengths from experiments, simulations and closed form solution are agreeing. The closed form expression {24} for wavelength developed using energy theory, involves the material properties in CMD. The web under tension in MD has very small stresses in CMD, with no change in CMD material properties, thereby making the wavelength expression valid even in the inelastic region.

The graphs below are representing amplitudes for the three test spans from experiments, simulation and closed form expression.

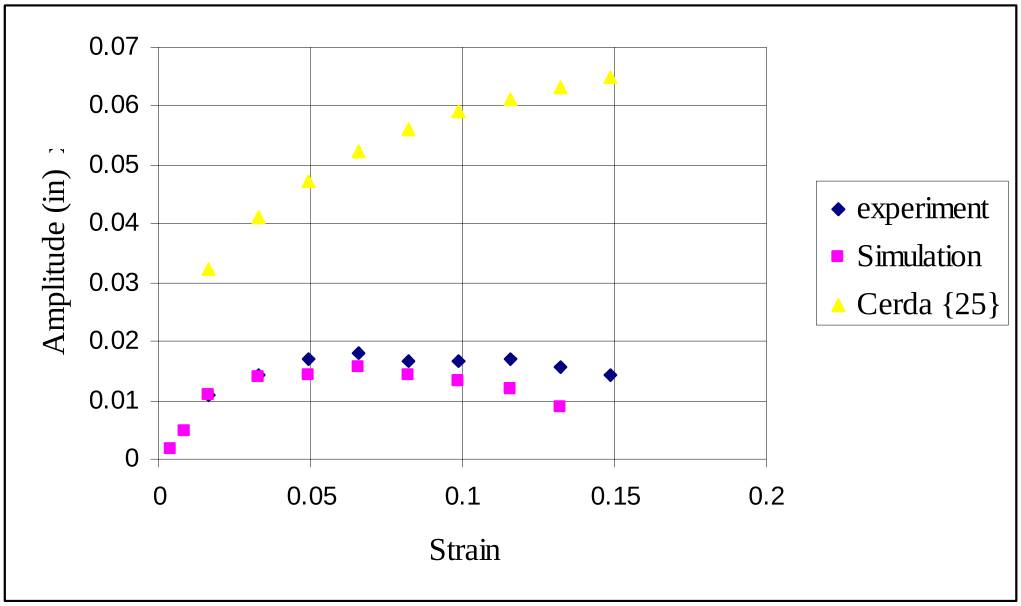

Figure 5.12-Amplitudes of the out-of-plane deformation in a 24 in test specimen

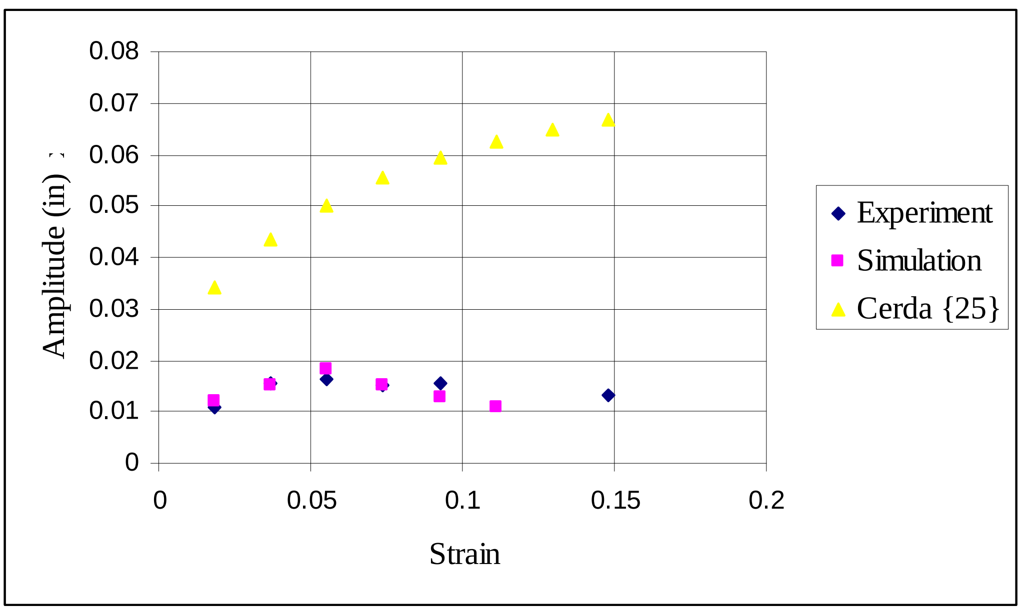

Figure 5.13-Amplitude of Out-of-plane Deformation in 27” Test Specimen

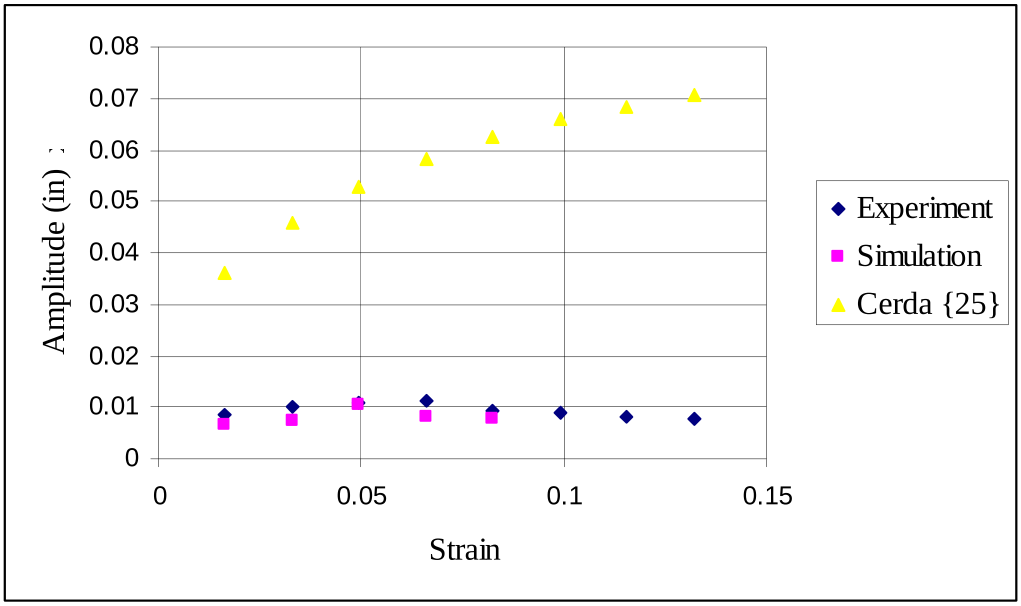

Figure 5.14-Amplitudes of the out-of-plane deformation in a 30 in test specimen

Since the expression for amplitude given by Cerda was agreeing neither with the Simulation results nor with the experiments, validation of Cerda's expression can be questioned. It appeared that his expression for amplitude was an developed by integrating the transverse inextensibility constraint along both length and width. The results from experiments as well as simulations can only be obtained and compared at a particular position along the length. Therefore in order to obtain an expression for average amplitude along the width I developed an expression by integrating inextensibility condition along the width at X=L/2, where X is the variable representing along the length and L is the total length of the test specimen.

$$\int_0^b \left[\frac{1}{2}\left(\frac{dw}{dy}\right)^2 - \frac{\Delta(x)}{w} \right] dy = 0 \qquad \{29\}$$

Substituting

$$w = A\,Sin\left(\frac{\pi x}{L}\right)Sin\left(\frac{n\pi y}{b}\right) \qquad \left(\frac{\partial w}{\partial y}\right)^2_{x=L/2} = \frac{A^2 n^2 \pi^2}{b^2} Cos^2\left(\frac{n\pi y}{b}\right)$$

and integrating the equation {29} will yields

$$A = \frac{2L\sqrt{\nu\gamma b}}{\pi^2\left[b^2 + 4n^2L^2\right]^{1/4}} \qquad \{30\}$$

Substituting the value of $\lambda = \sqrt{2\pi L t}\sqrt[4]{\frac{1}{3(1-\nu^2)\gamma}}$

$$A = \frac{2L\sqrt{\gamma\nu}}{\pi\left(1 + \frac{12L^2\gamma\left(1-\nu^2\right)}{t^2\pi^2}\right)^{1/4}} \qquad \{31\}$$

The graphs below represents the amplitudes from experiments, simulation and from the new expression {31} developed for the three different test spans.

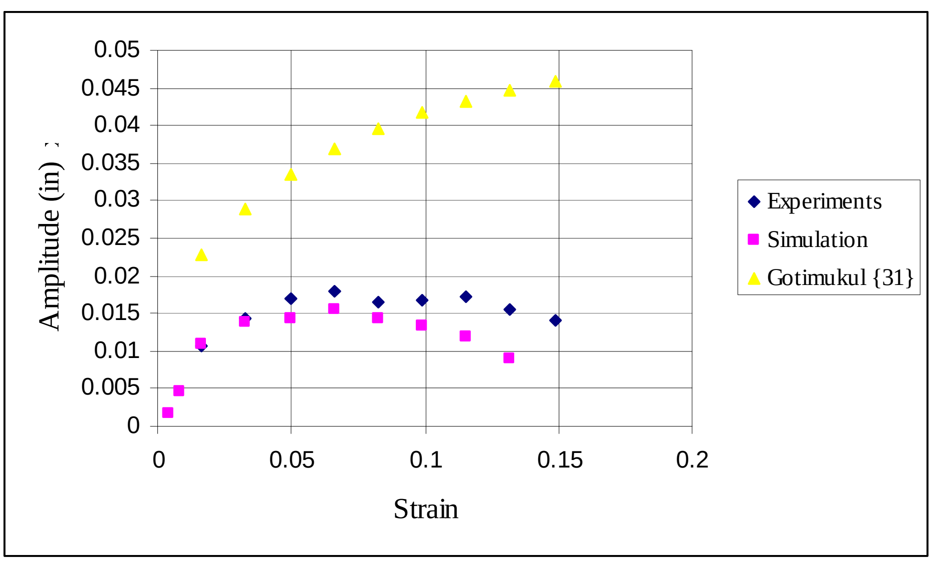

Figure 5.15-Amplitudes of 24” Test Specimen

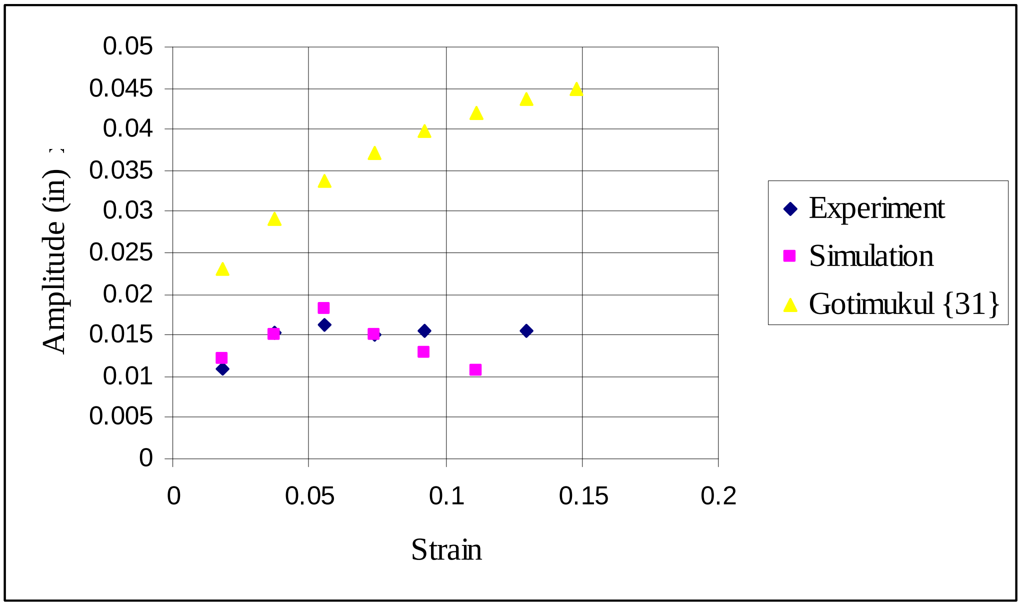

Figure 5.16-Amplitudes of 27” Test Specimen

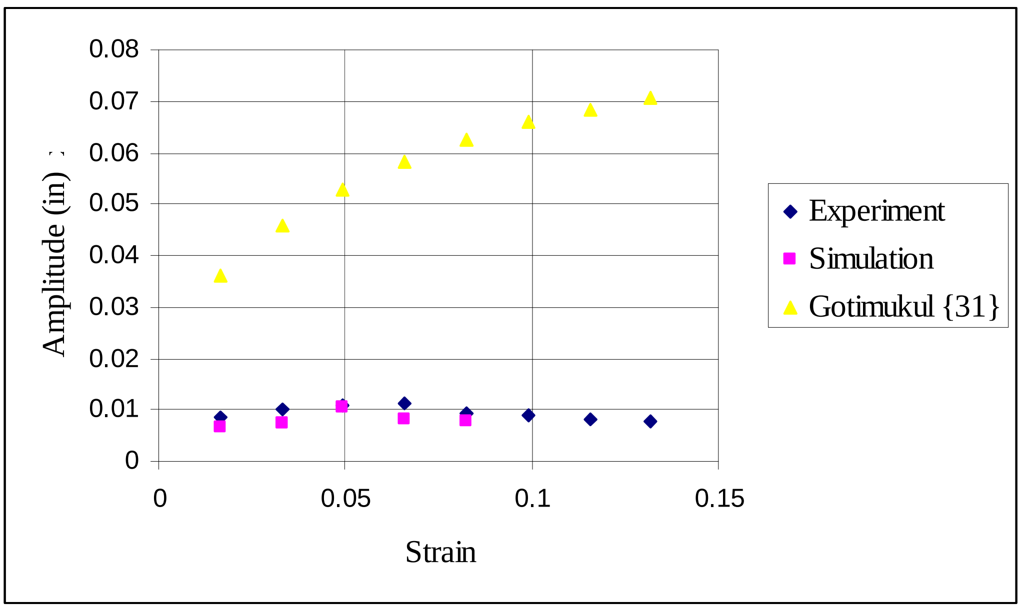

Figure 5.17-Amplitudes of 30” Test Specimen

From the above graphs we can concur that the new expression developed by averaging the out-of-plane deformation along the width alone is not in good agreement with the results from experiments and simulation but it can be proclaimed that it's better than that of Cerda's expression.

In order to see the effect of the inelastic material properties on the closed form expression for average amplitude along the width, it was expressed in stress and tangent modulus.

The expression {31} for amplitude was modified by expressing strain in terms of Modulus and stress.

$$A = \frac{2L\sqrt{\gamma\nu}}{\pi\left(1 + \frac{12L^2\left(\sigma/E_T\right)\left(1-\nu^2\right)}{t^2\pi^2}\right)^{1/4}} \qquad \{32\}$$

The tangent modulus (E_T) used in developing the results was obtained from the Table 3.1 Stress (σ) from the load obtained from load cell and Poisson's ratio from the expression {28}.

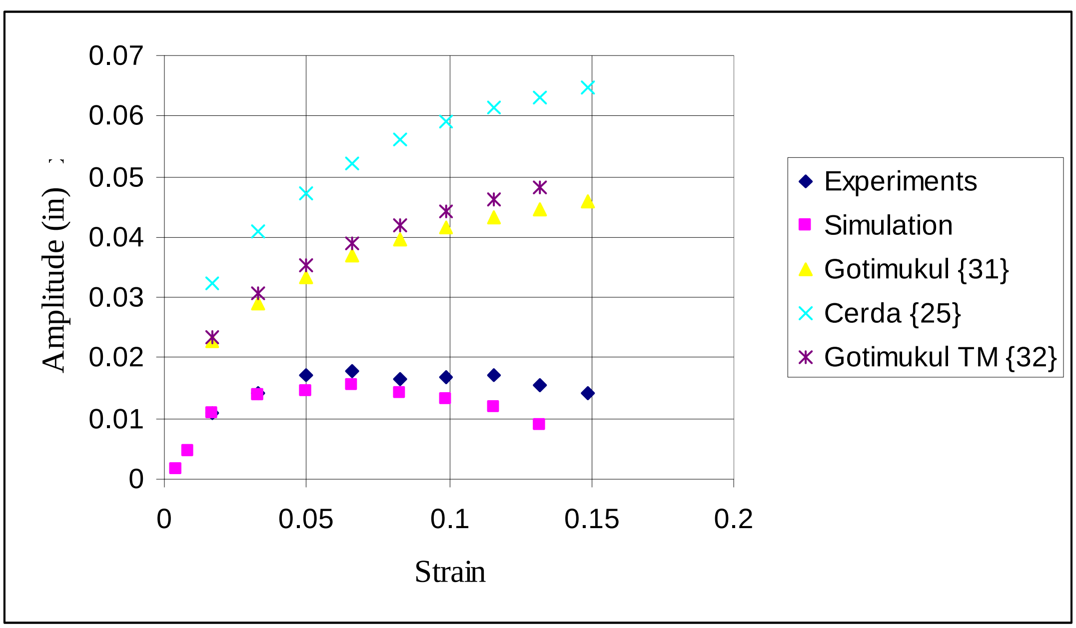

Figure 5.18-Amplitudes of 24" test specimen with inelastic material properties

It can be inferred from the graph that using the expression in terms of inelastic material properties would still predict the amplitudes to be of the same order which is contradicting the experimental and simulation results.

CHAPTER V

CONCLUSIONS

Experiments were conducted on a polyethylene web to study the behavior of the troughs, at different strains both in linear and non linear range. The conclusions drawn from this research includes

1. From the figures 5.8, 5.9, 5.10 it can be concluded that the closed form expression {24} for wavelength of the troughs claimed by Cerda is capable of predicting the wavelength for strain range of 0.0165 to 0.166. These strains proceed well into the plastic range. However the CMD modulus enters expression {24} and the stresses in this direction are small.

2. From the figures 5.12 - 5.17 it appears that the two closed form expressions {24} and {31} for average amplitude of troughs developed by Cerda and Gotimukul are not in agreement with the experiment and simulation results. They do however help over estimate the amplitude of the troughs. Gotimukul overestimates by a factor of ~ 2.5 and Cerda overestimates by a factor of ~ 3.6. This conclusion is applicable only in the linear elastic range.

3. Neither of the two closed form solutions is accurate in predicting the amplitudes of the troughs in both linear as well as non linear region.

Future Work:

It has been shown in this research that wavelength of the troughs on a web can be predicted, but prediction of amplitudes in both elastic and inelastic region is still in the ambiguity. Further research can be done in developing a closed form solutions, not based on linear energy theory, which can predict the amplitudes of the trough.

REFERENCES

[1] S.Timoshenko, S.P., Gere, J.M., Theory of Elastic Stability, 2nd edition McGraw-Hill, 1961, p.324-332.

[2] Good, J.K, and Biesel, J.A, “Instability of Webs: The Prediction of Troughs and Wrinkles” Advances in Pulp and Paper Research Oxford 2009 Vol 1 pp 517

[3] Cerda, E, Ravi-Chandar, E and Mahadevan, L “Wrinkling of an Elastic Sheet Under Tension” Nature Publishing Group 2002 and pp 419-579.

[4] Cerda, E, Mahadevan, L “Geometry and Physics of Wrinkling” The American Physical Society 2003 Vol 90, No. 7 and pp 074302-1 – 074302-4

APPENDICES

The experiments were conducted on different test spans at different strain levels, in the results chapter, the out of plane deformation at two strain levels were shown. The out of plane deformation of the test specimens at other strain levels are shown below.

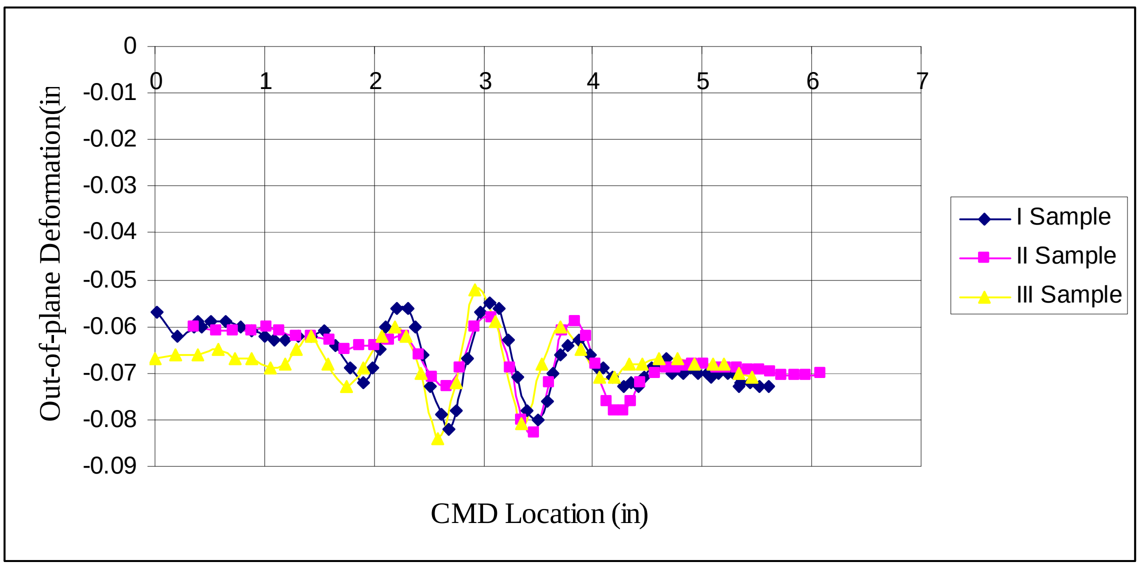

Out-of-plane deformation of three different 24” test specimen at a strain of 0.0165

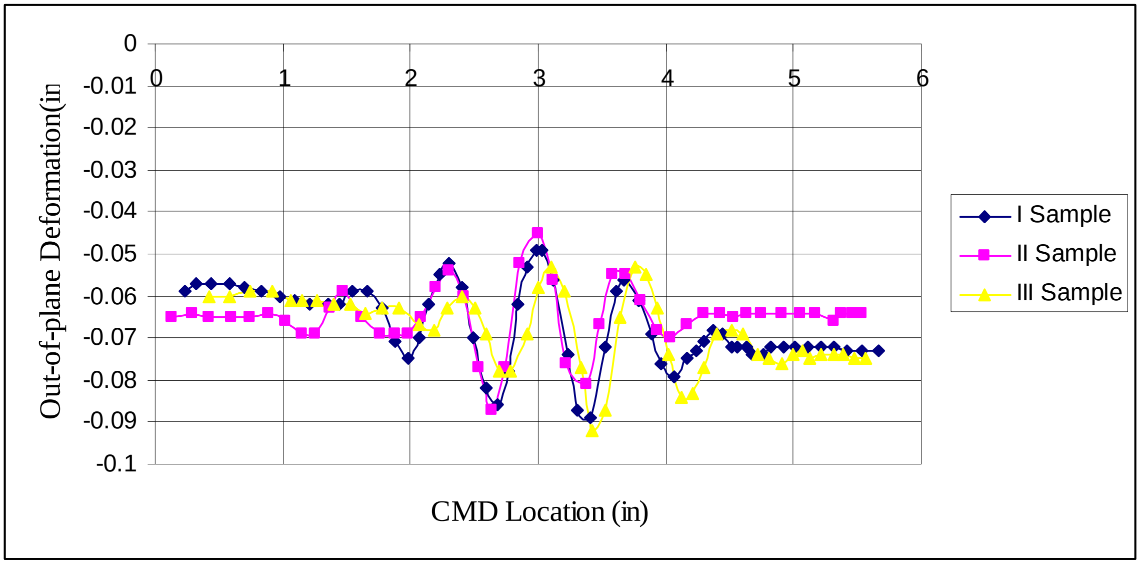

Out-of-plane deformation of three different 24" test specimen at a strain of 0.033

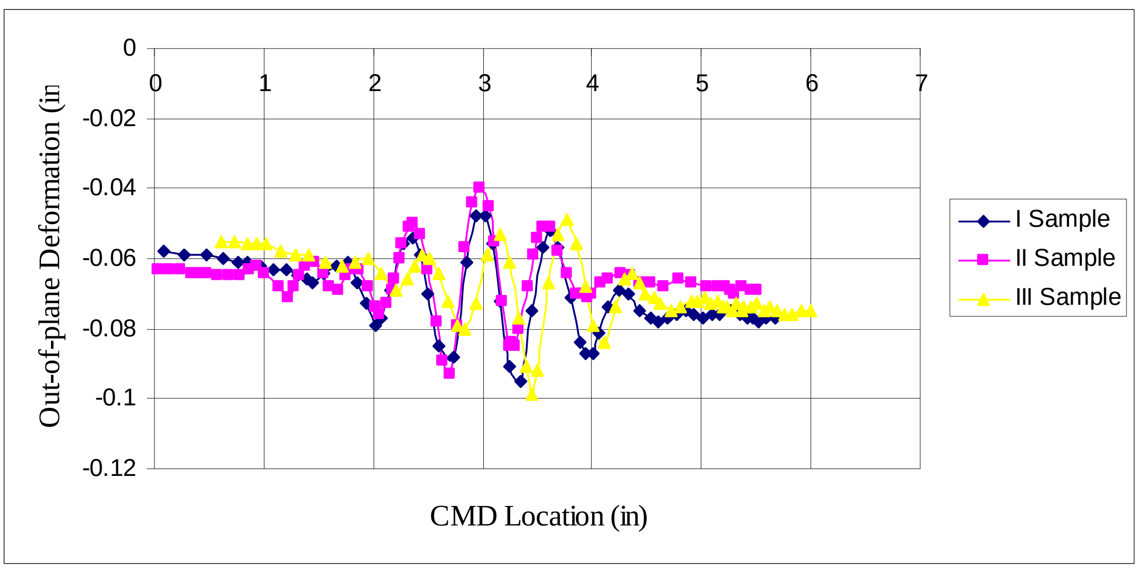

Out-of-plane deformation of three different 24" test specimen at a strain of 0.0495

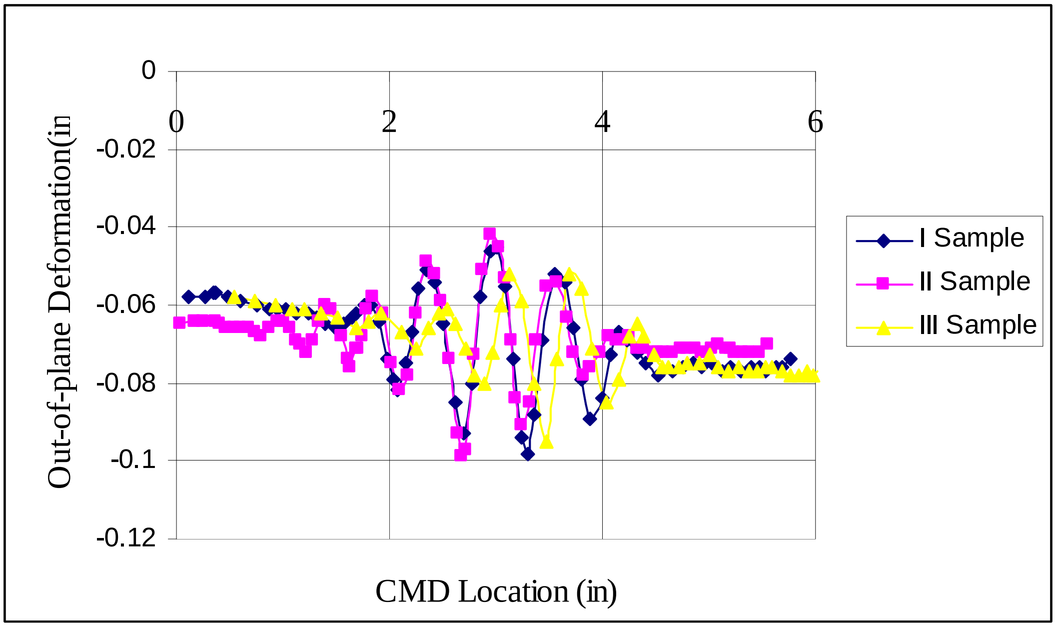

Out-of-plane deformation of three different 24" test specimen at a strain of 0.066

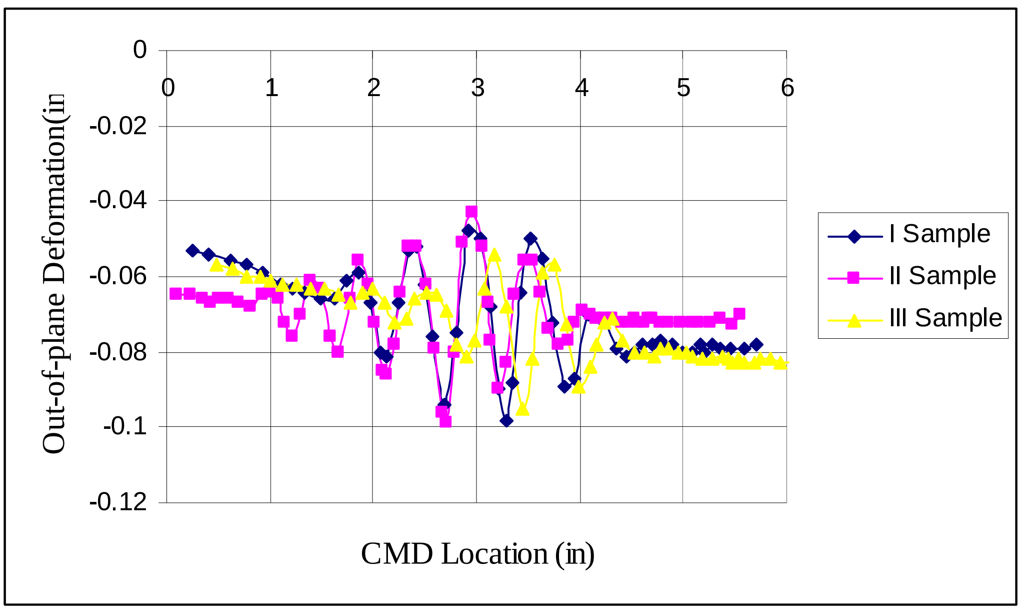

Out-of-plane deformation of three different 24" test specimen at a strain of 0.0825

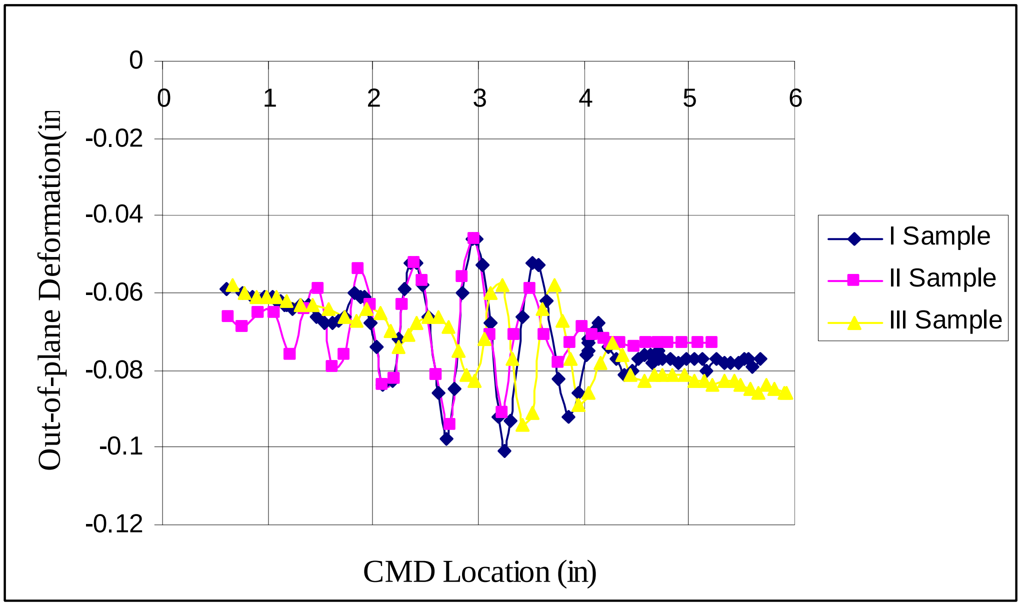

Out-of-plane deformation of three different 24" test specimen at a strain of 0.099

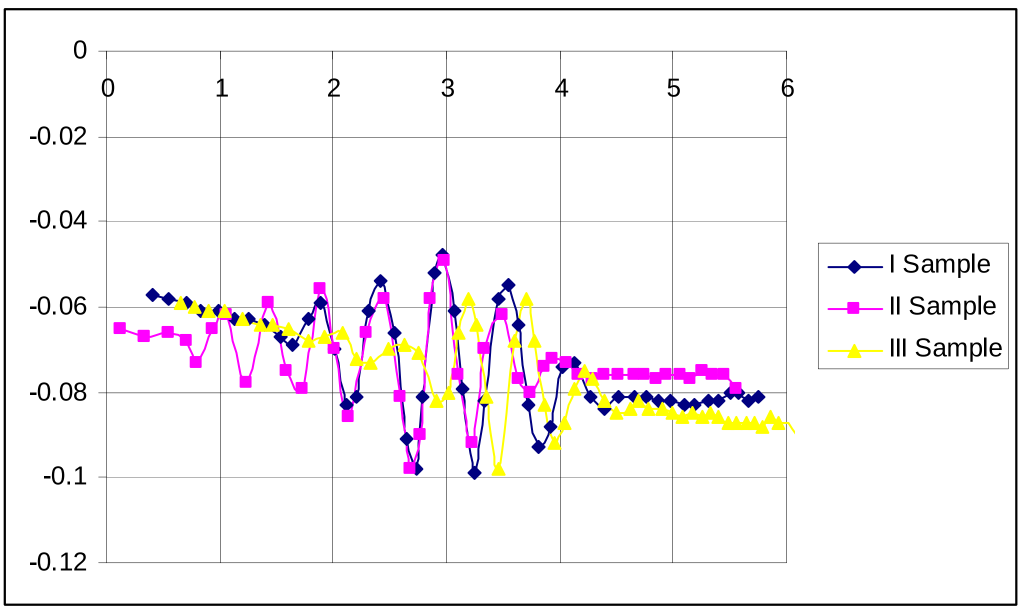

Out-of-plane deformation of three different 24" test specimen at a strain of 0.1155

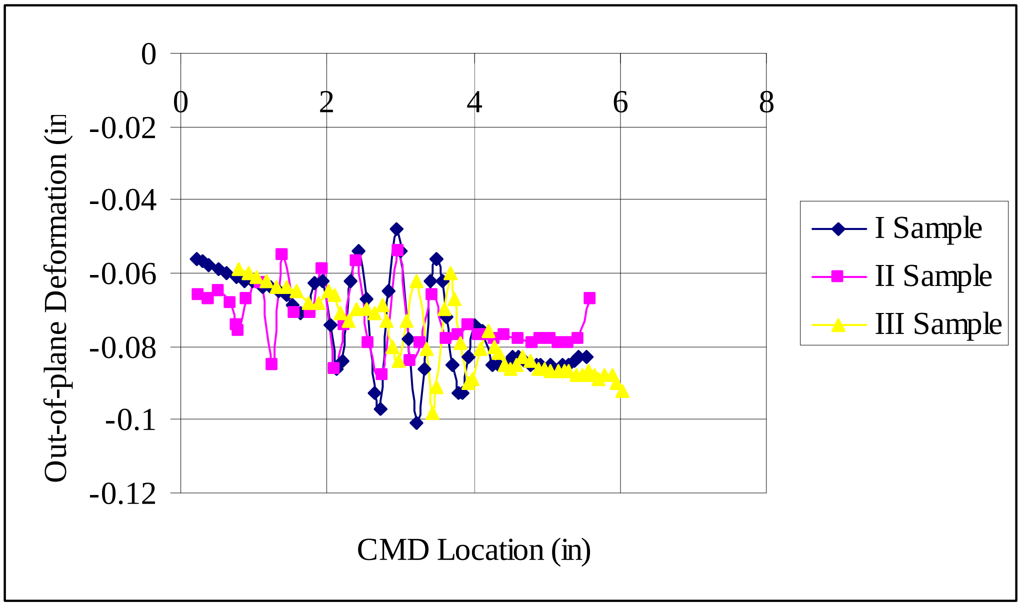

Out-of-plane deformation of three different 24” test specimen at a strain of 0.132

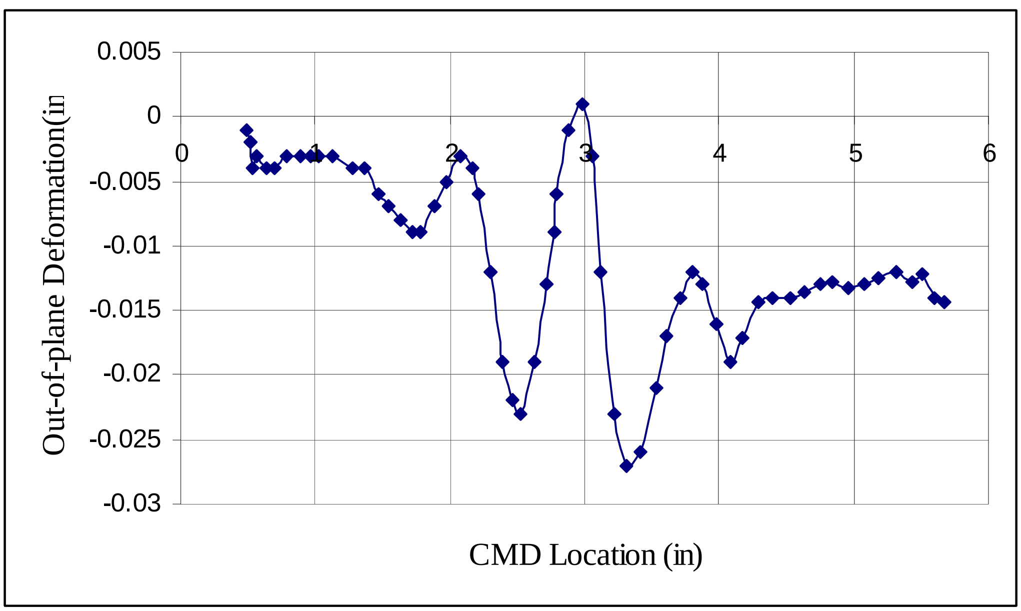

Out-of-plane deformation of 27” test specimen at a strain of 0.0185

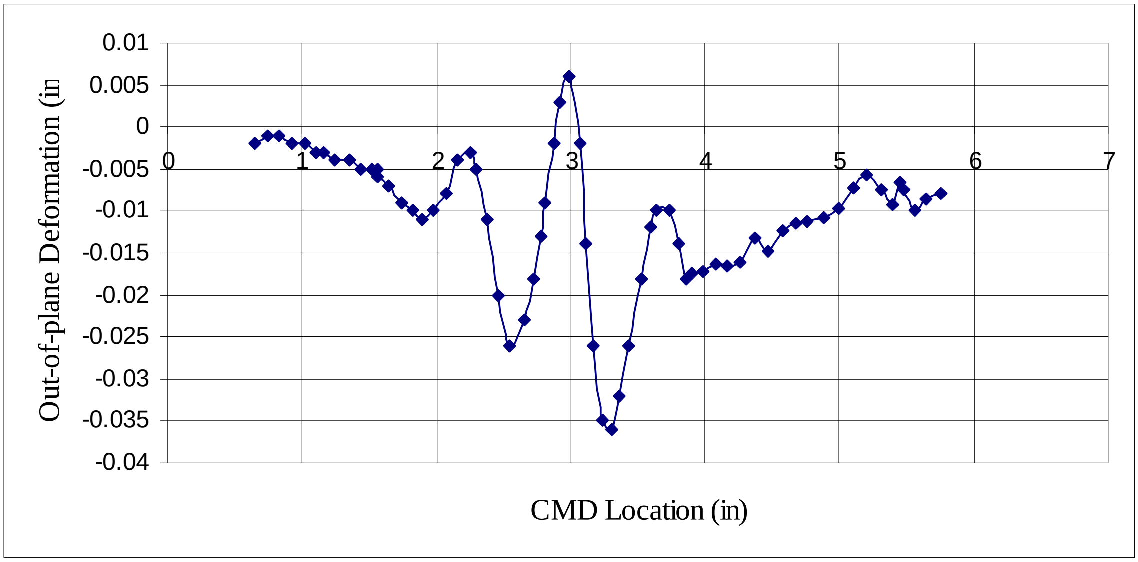

Out-of-plane deformation of 27” test specimen at a strain of 0.037

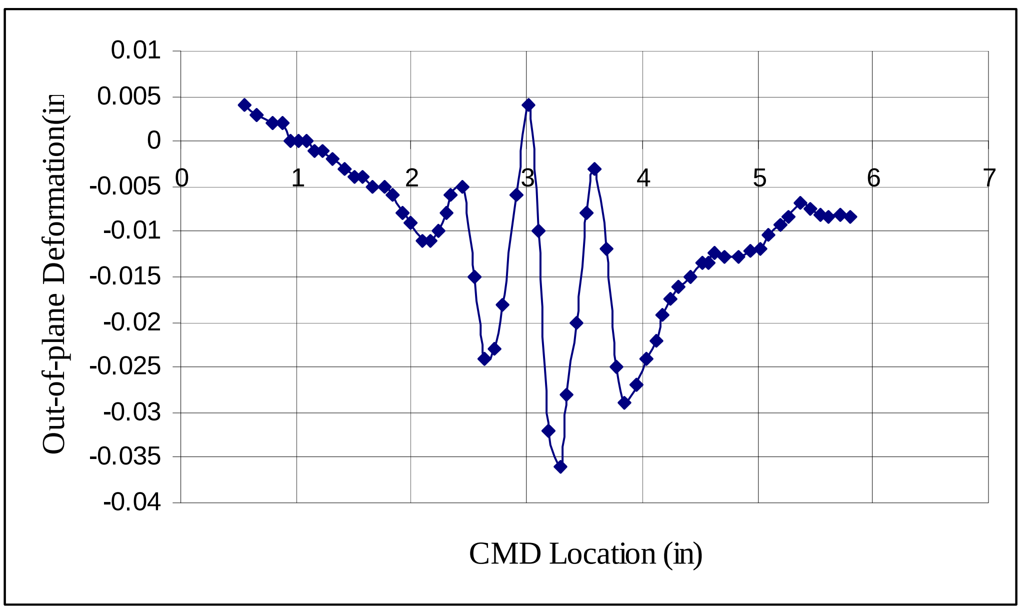

Out-of-plane deformation of 27” test specimen at a strain of 0.0555

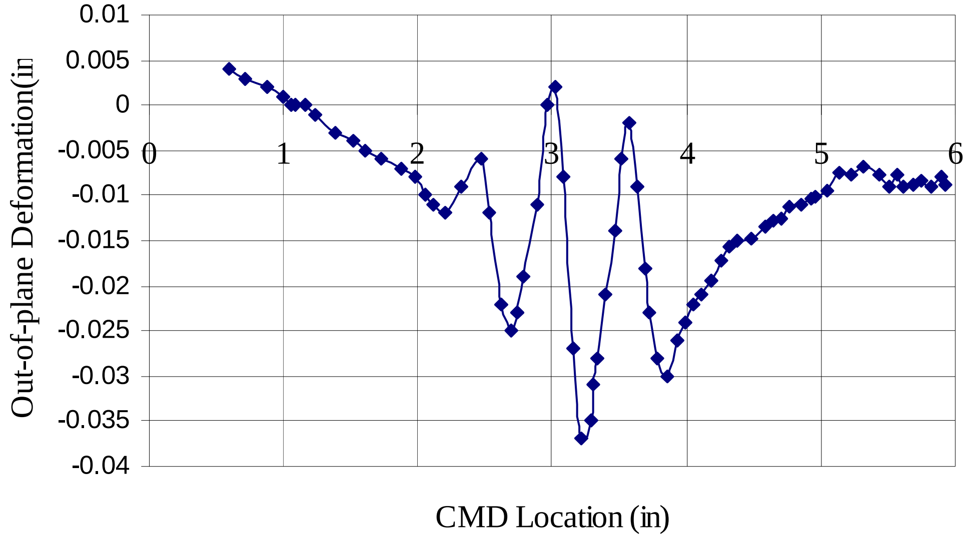

Out-of-plane deformation of 27” test specimen at a strain of 0.074

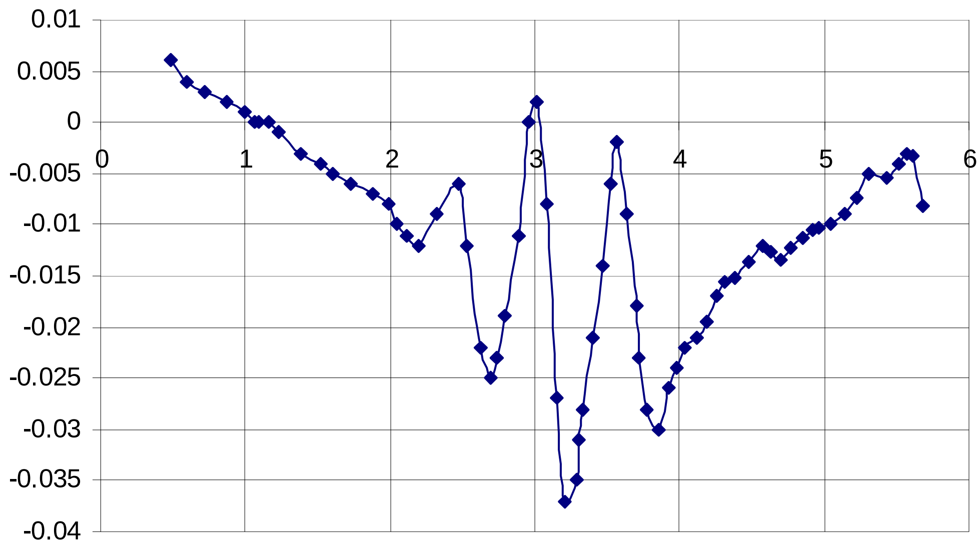

Out-of-plane deformation of 27” test specimen at a strain of 0.0925

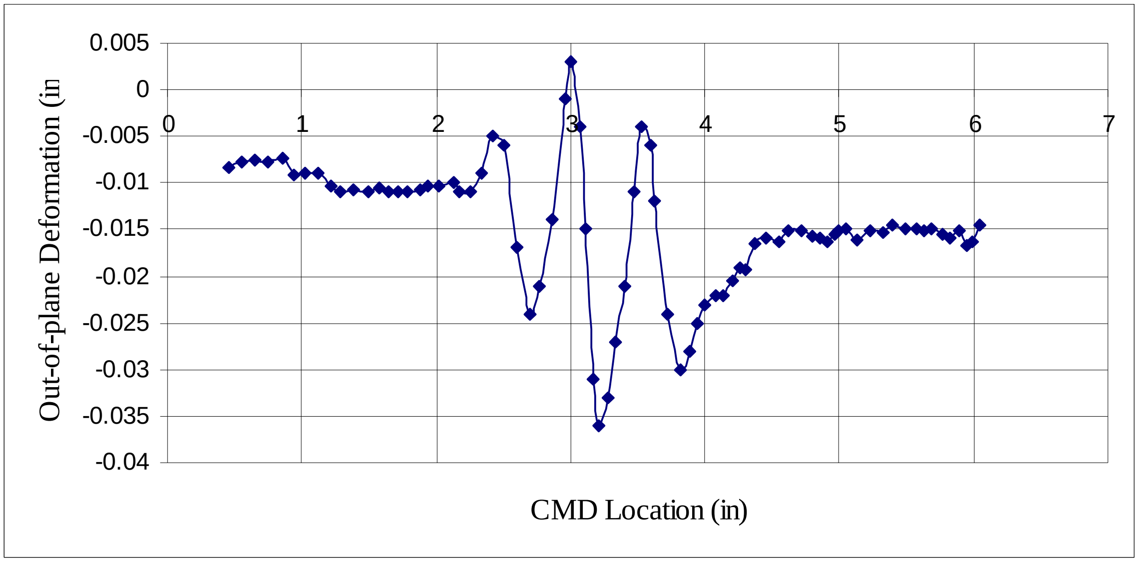

Out-of-plane deformation of 27” test specimen at a strain of 0.111

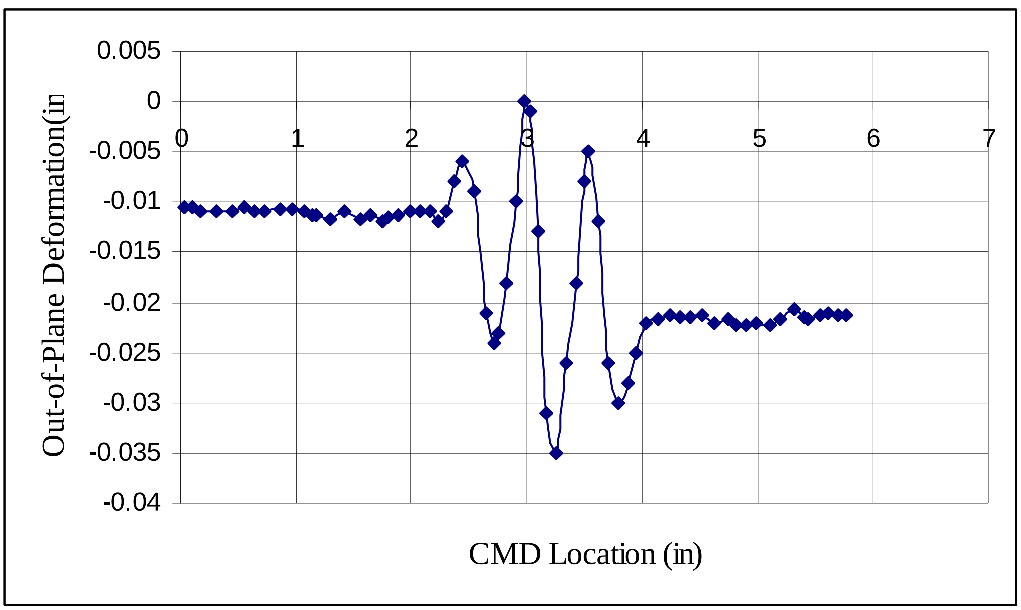

Out-of-plane deformation of 27” test specimen at a strain of 0.1296

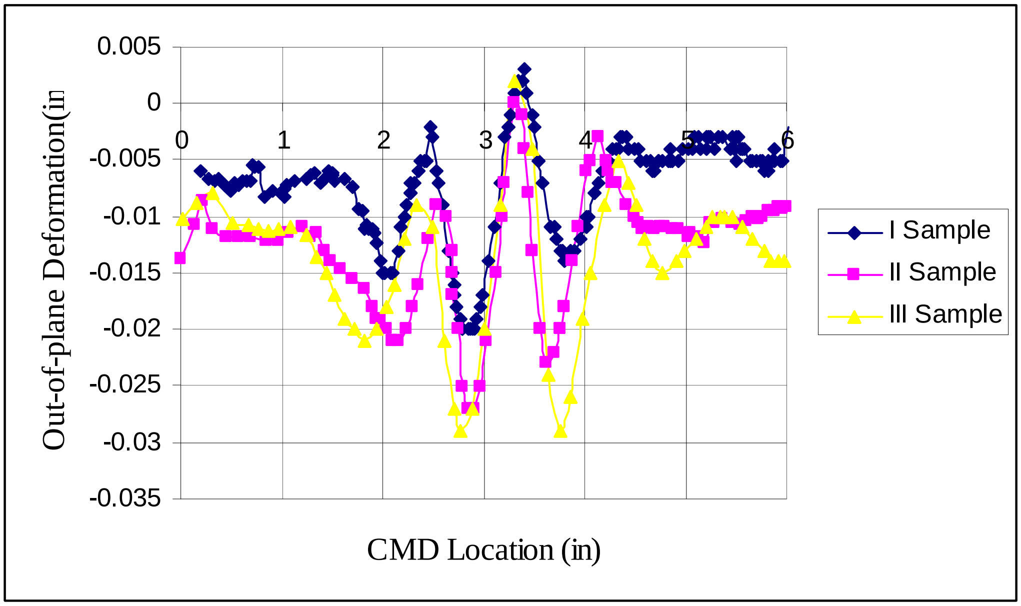

Out-of-plane deformation of three 30” test specimen at a strain of 0.0165

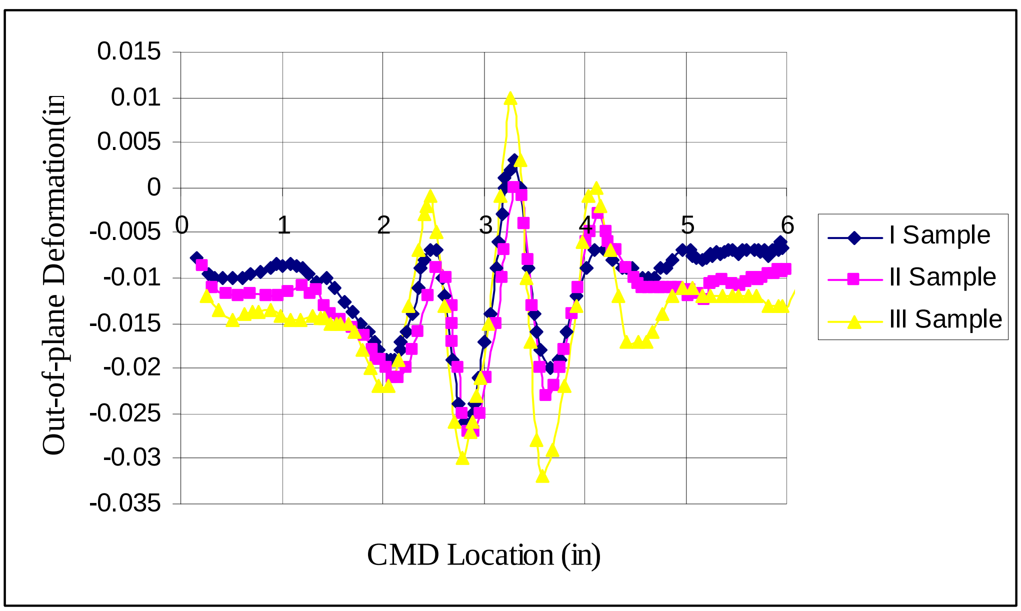

Out-of-plane deformation of three 30” test specimen at a strain of 0.033

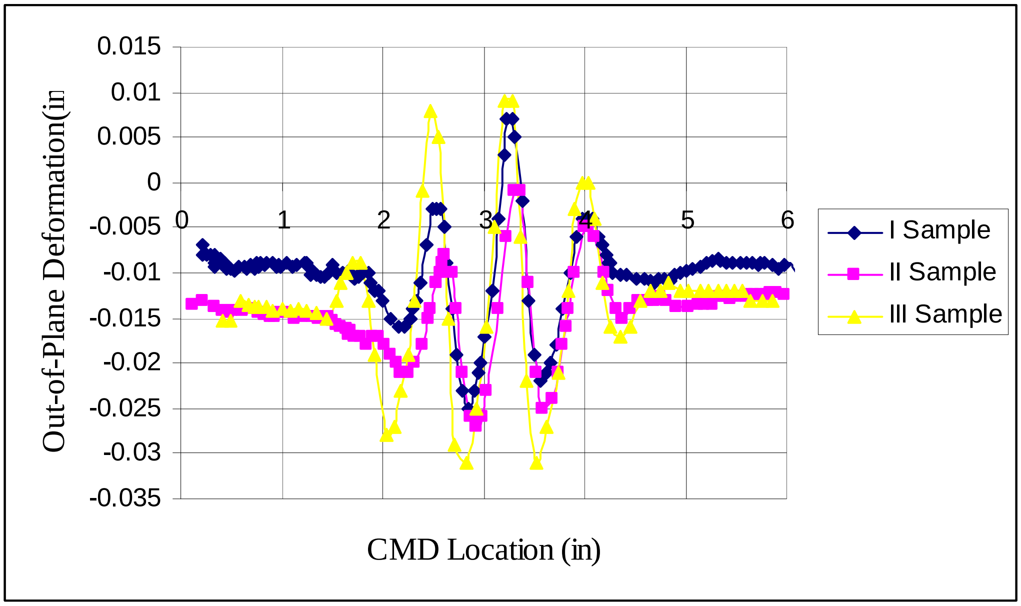

Out-of-plane deformation of three 30” test specimen at a strain of 0.0495

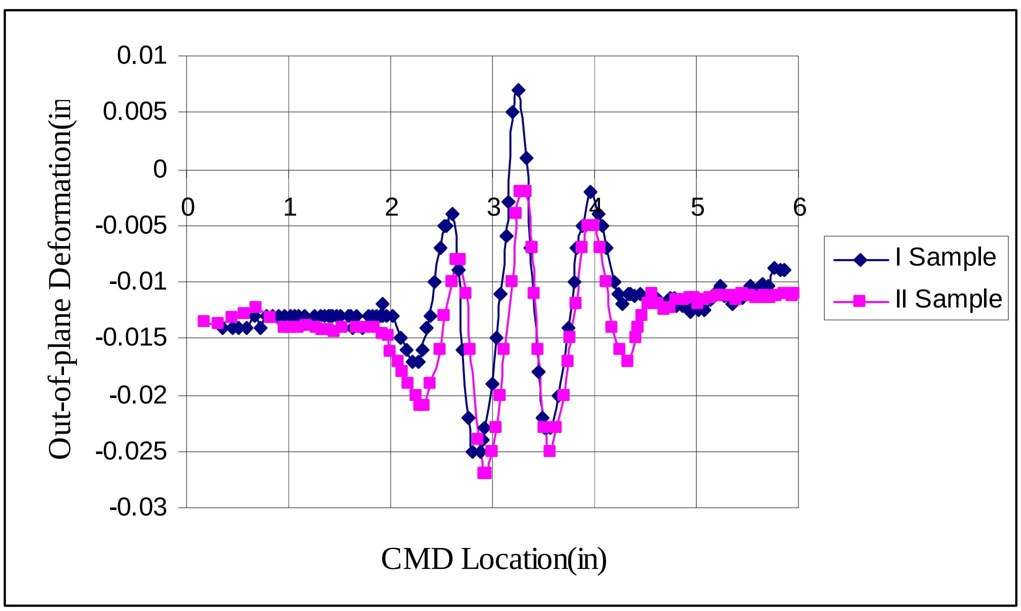

Out-of-plane deformation of two 30” test specimen at a strain of 0.066

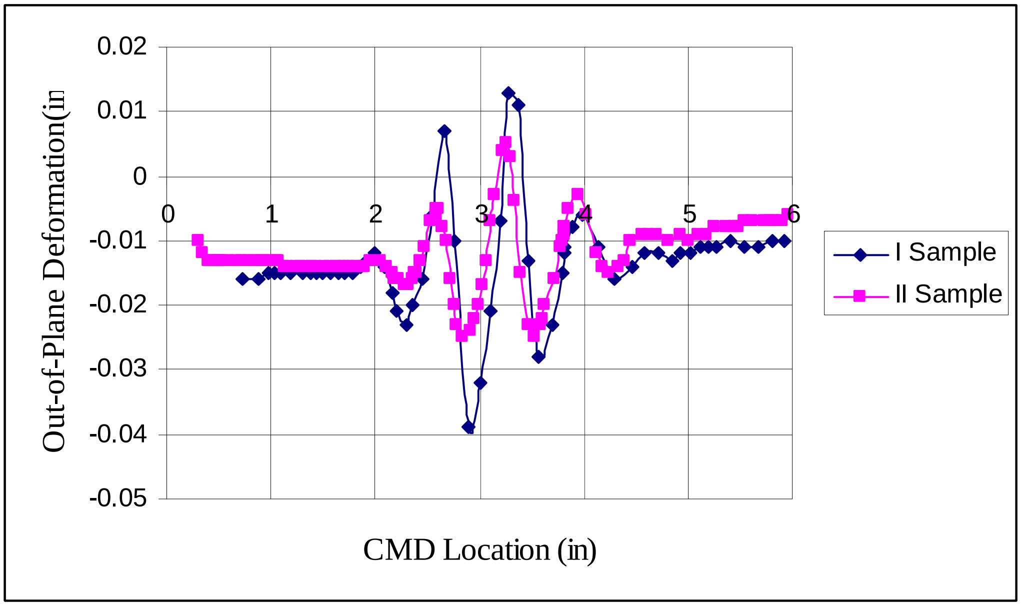

Out-of-plane deformation of two 30” test specimen at a strain of 0.0826

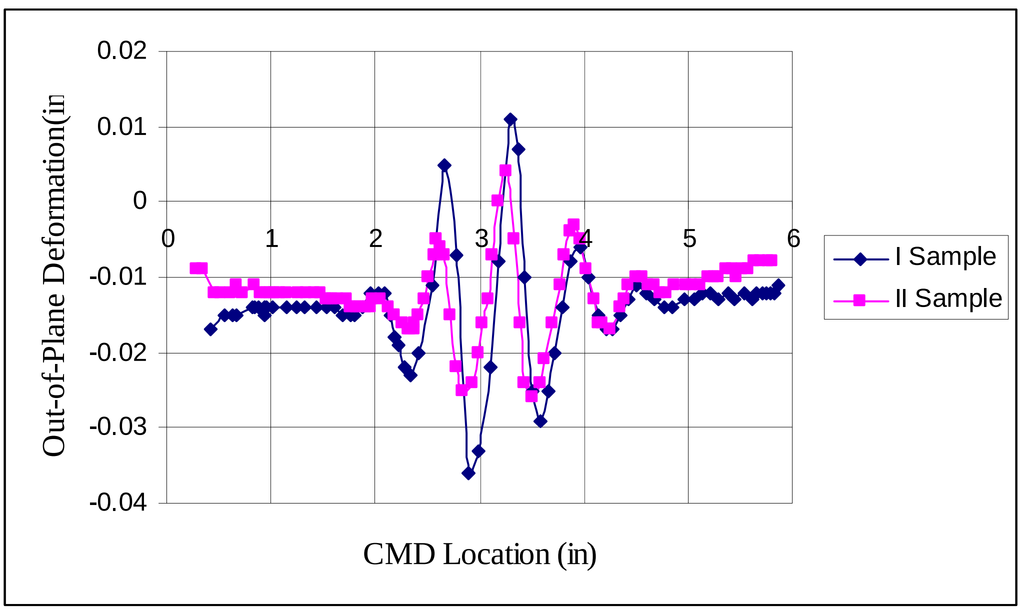

Out-of-plane deformation of two 30” test specimen at a strain of 0.099

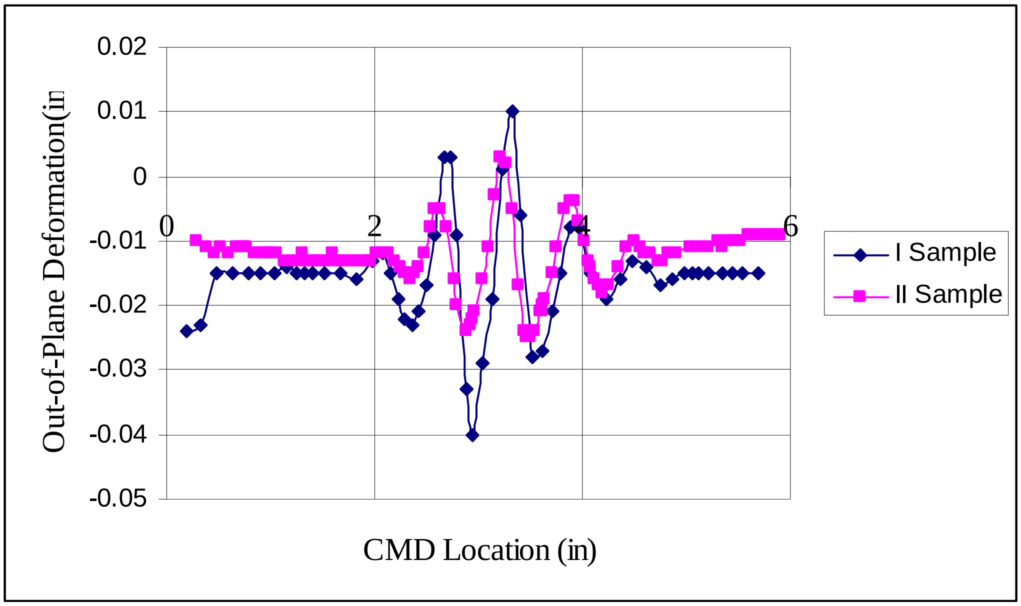

Out-of-plane deformation of two 30” test specimen at a strain of 0.1157

The Out-of-plane deformations of the test specimen of different lengths from ABAQUS simulations at different strains are shown below.

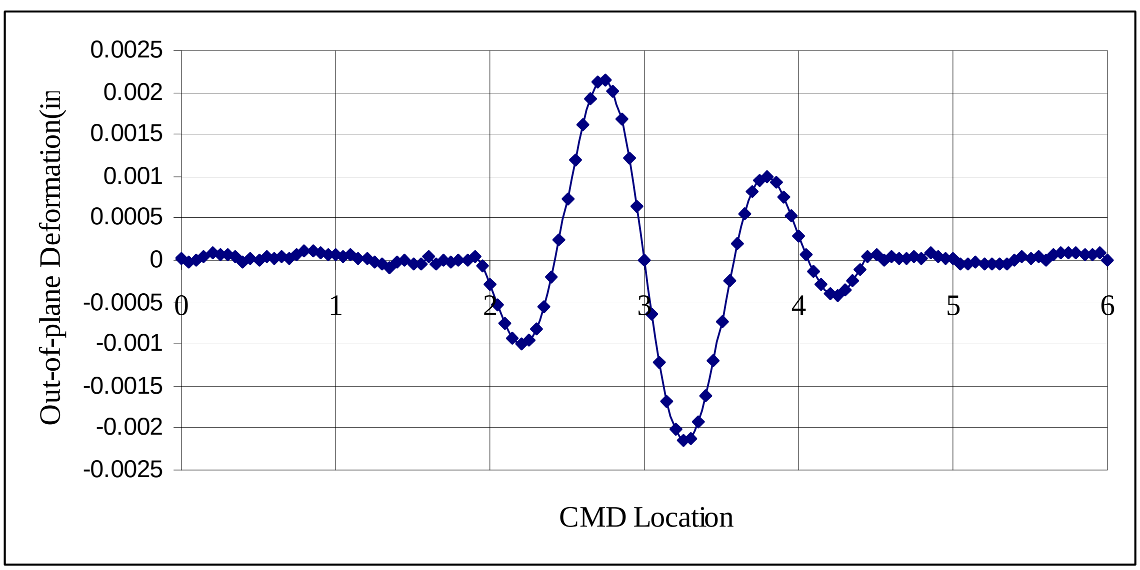

Out-plane-deformation of a 24” test specimen from simulation at a strain of 0.00467

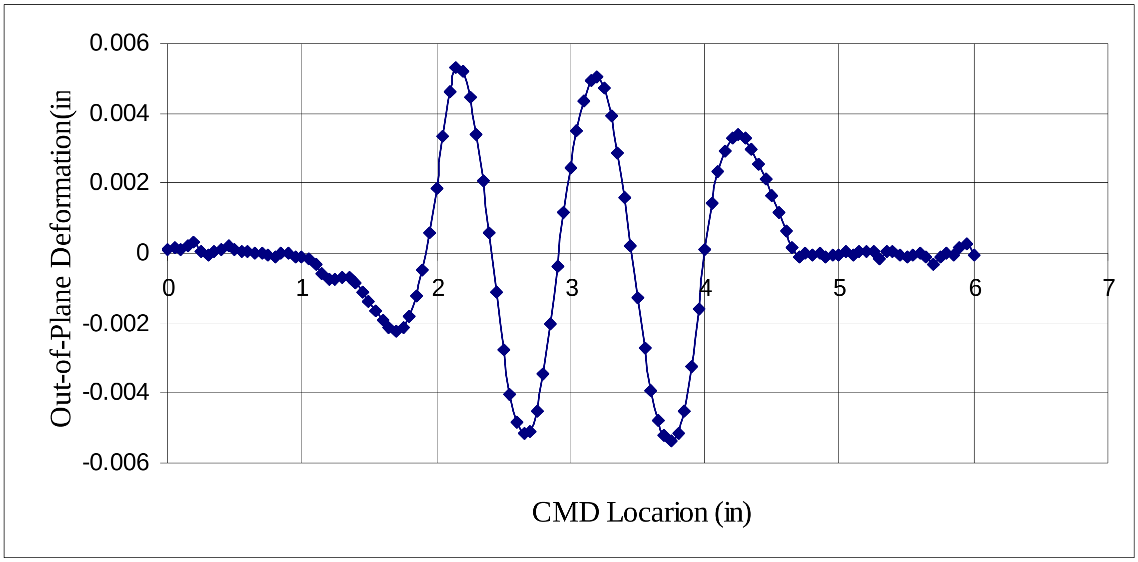

Out-plane-deformation of a 24” test specimen from simulation at a strain of 0.00834

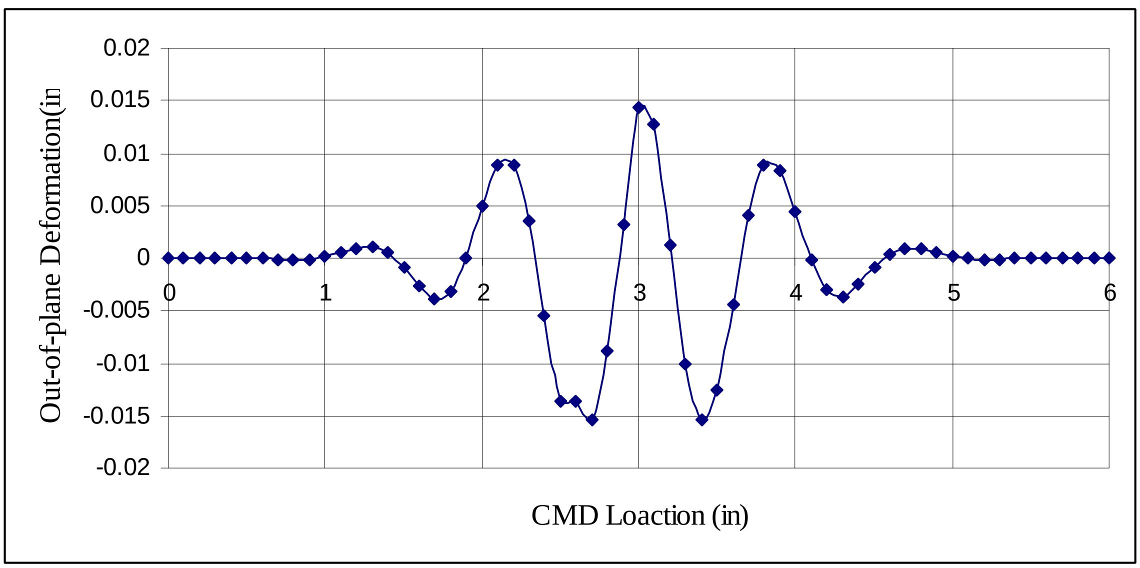

Out-plane-deformation of a 24” test specimen from simulation at a strain of 0.0165

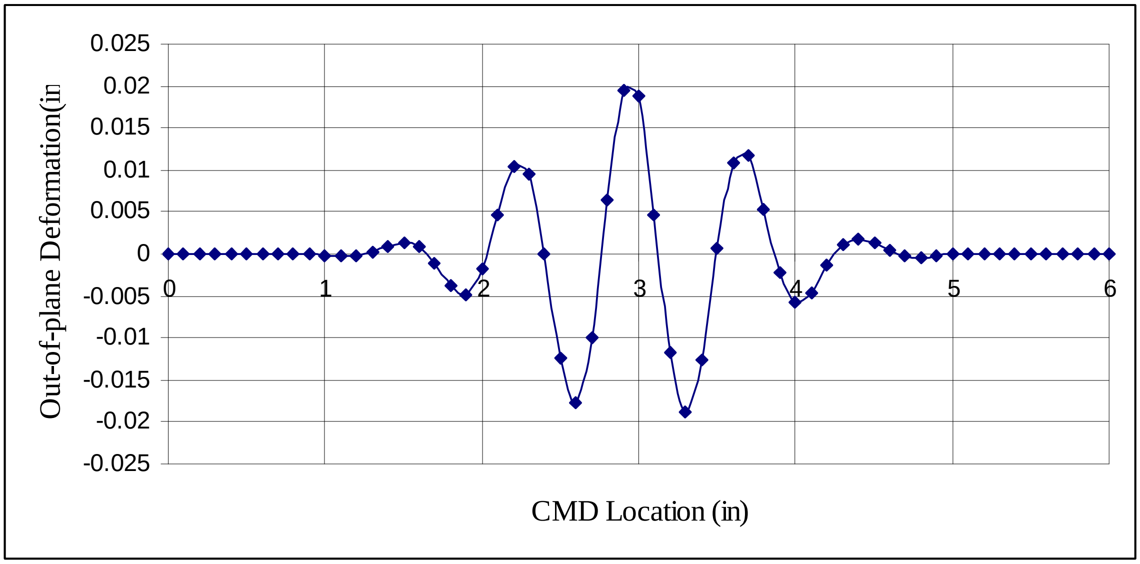

Out-plane-deformation of a 24” test specimen from simulation at a strain of 0.033

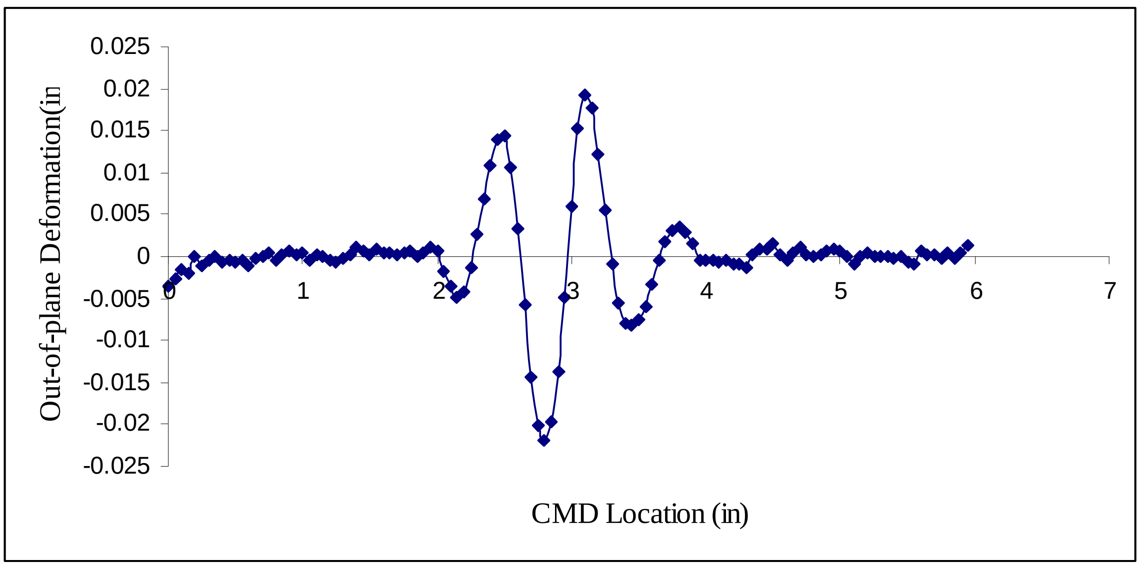

Out-plane-deformation of a 24” test specimen from simulation at a strain of 0.0495

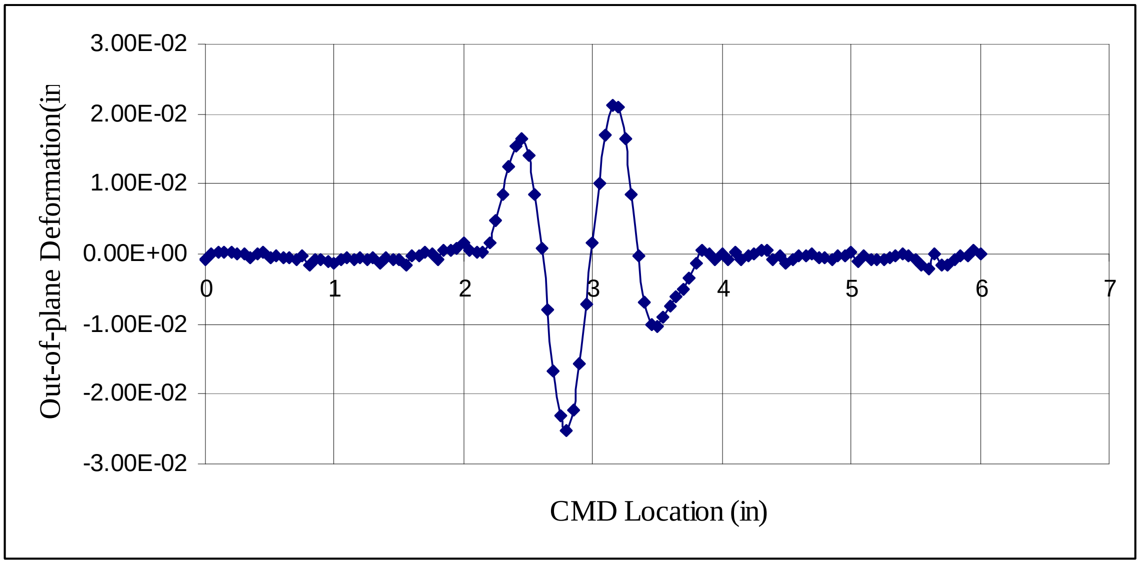

Out-plane-deformation of a 24” test specimen from simulation at a strain of 0.066

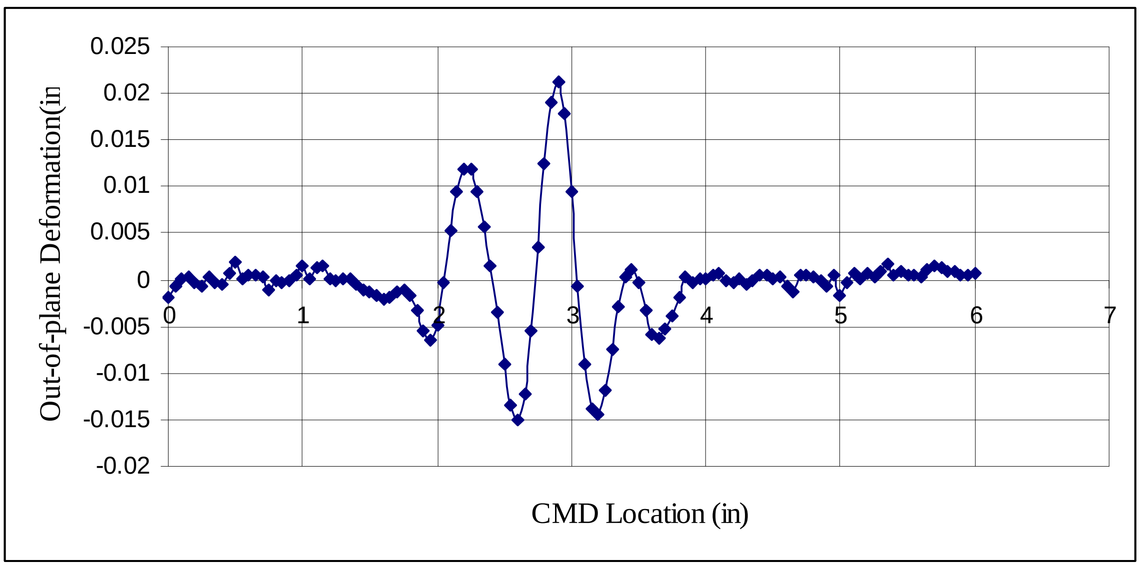

Out-plane-deformation of a 24” test specimen from simulation at a strain of 0.0825

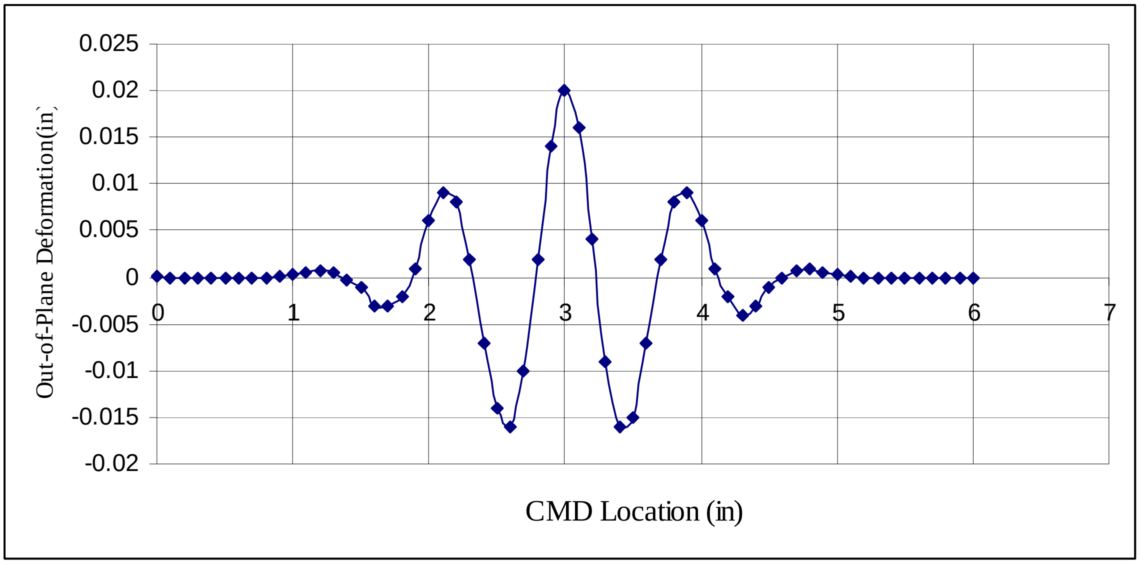

Out-plane-deformation of a 27” test specimen from simulation at a strain of 0.0185

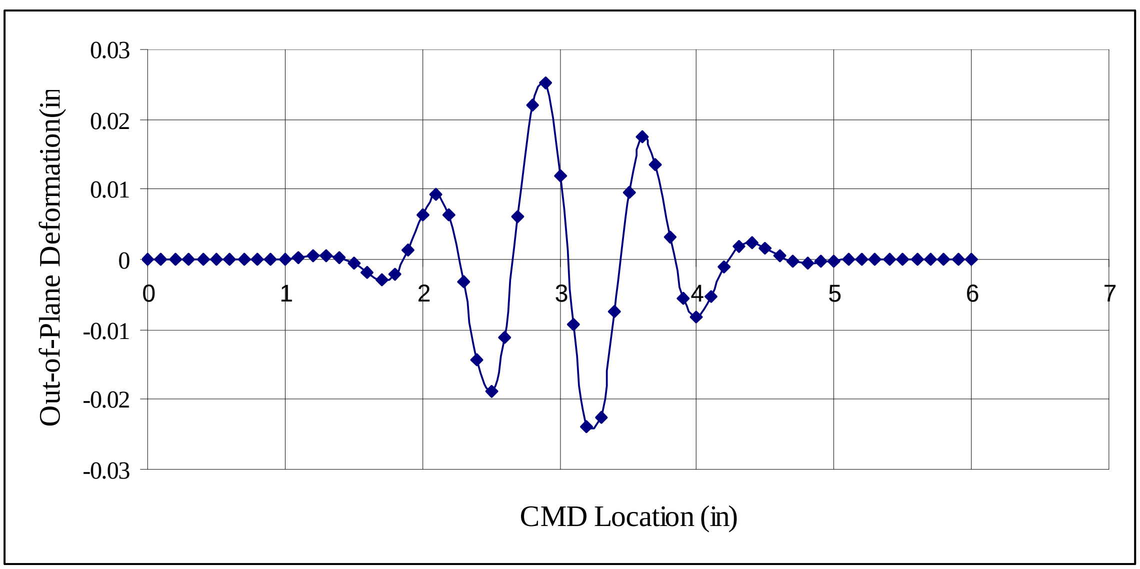

Out-plane-deformation of a 27” test specimen from simulation at a strain of 0.037

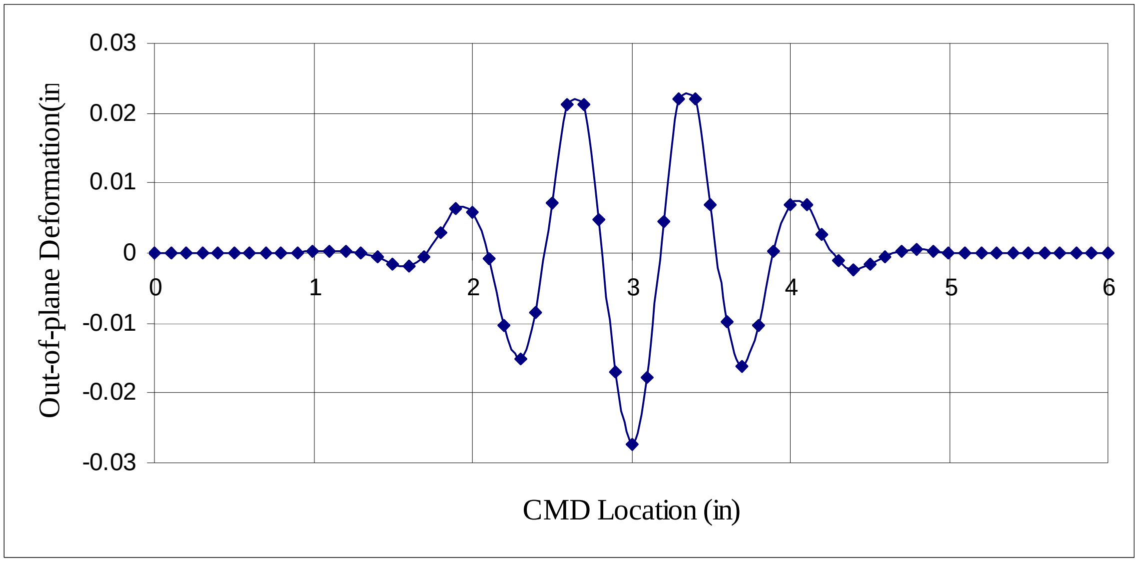

Out-plane-deformation of a 27” test specimen from simulation at a strain of 0.055

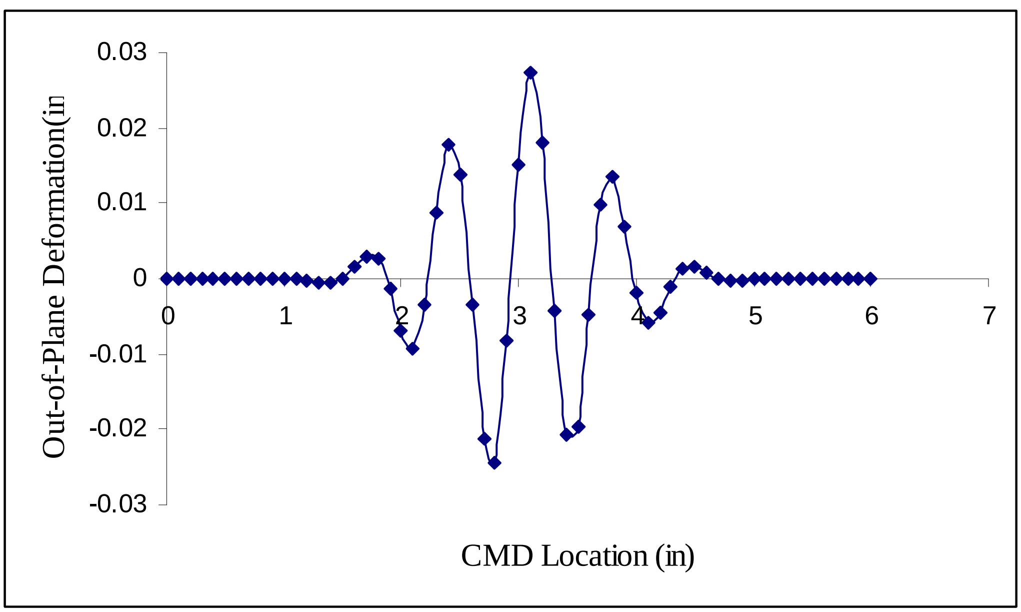

Out-plane-deformation of a 27” test specimen from simulation at a strain of 0.0747

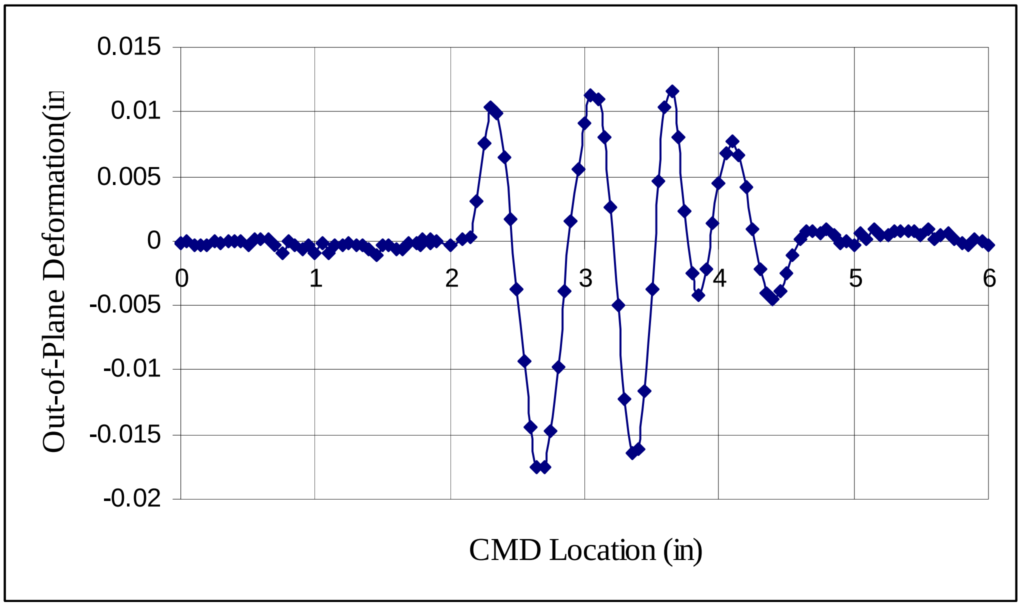

Out-plane-deformation of a 27” test specimen from simulation at a strain of 0.0925

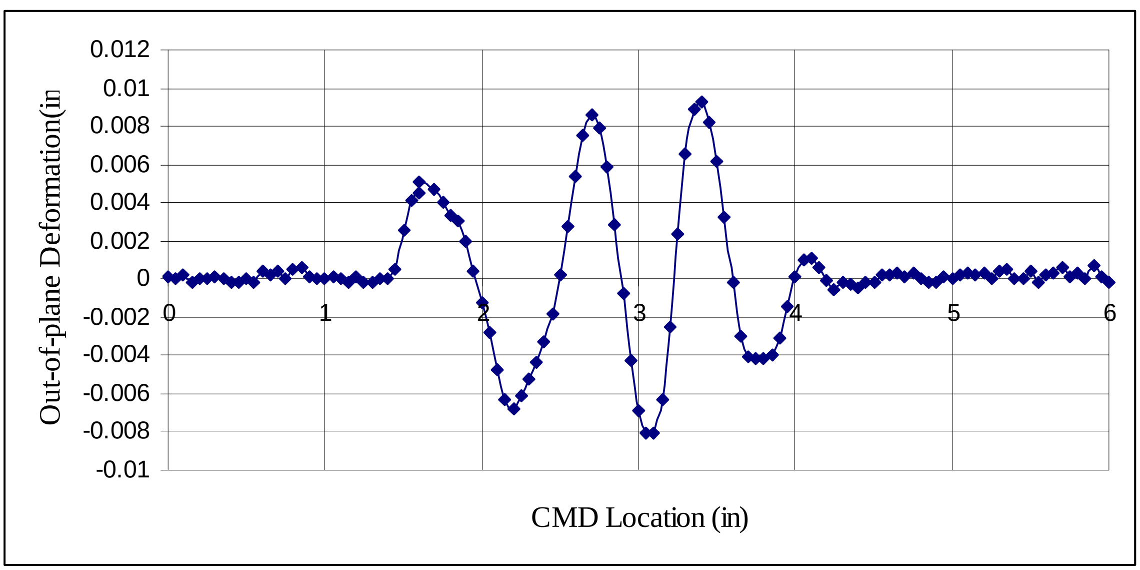

Out-plane-deformation of a 30” test specimen from simulation at a strain of 0.033

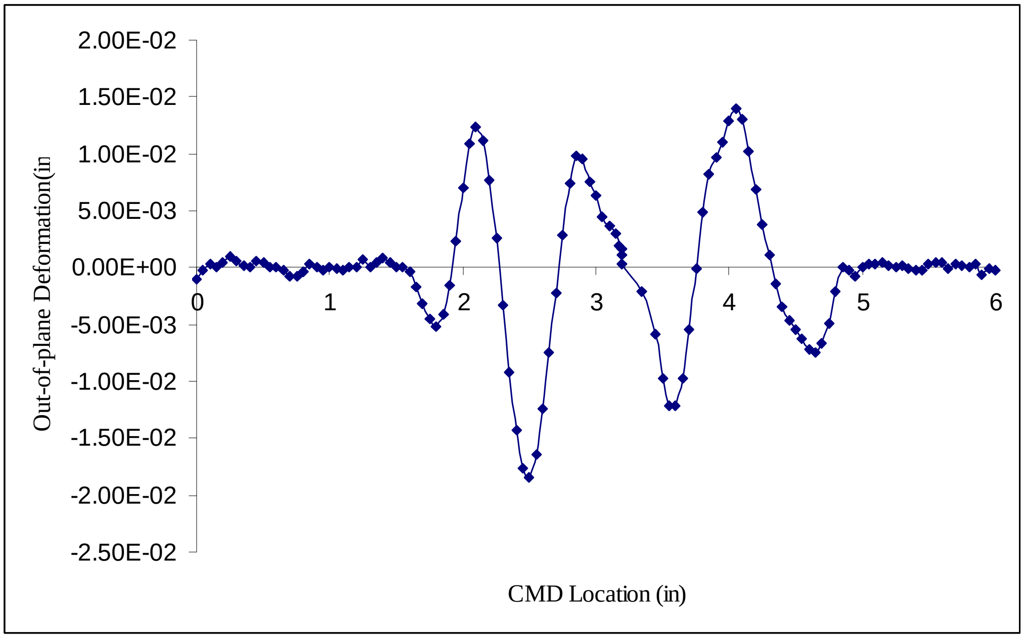

Out-plane-deformation of a 30" test specimen from simulation at a strain of 0.0495

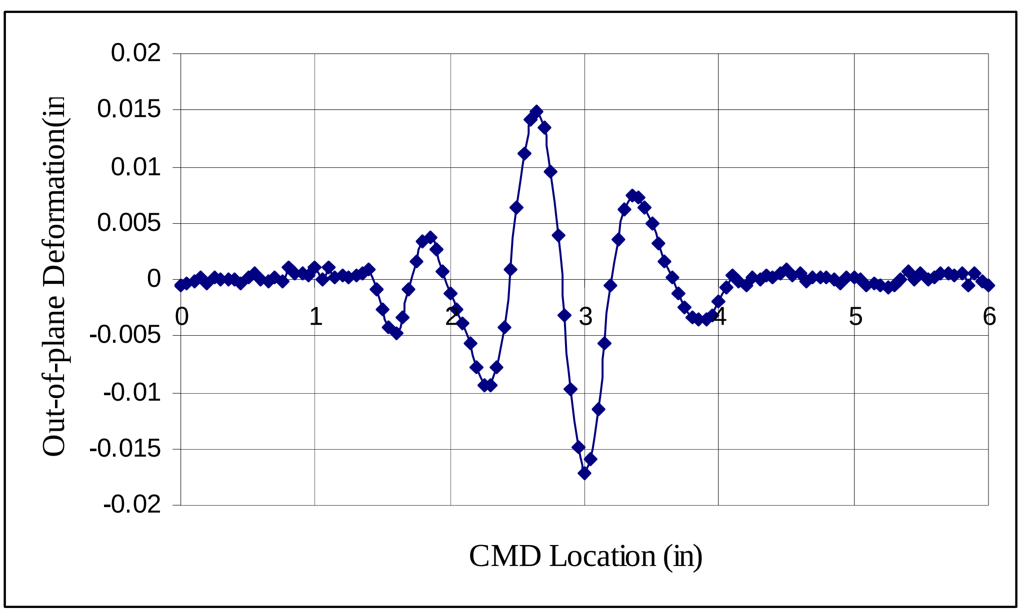

Out-plane-deformation of a 30" test specimen from simulation at a strain of 0.066

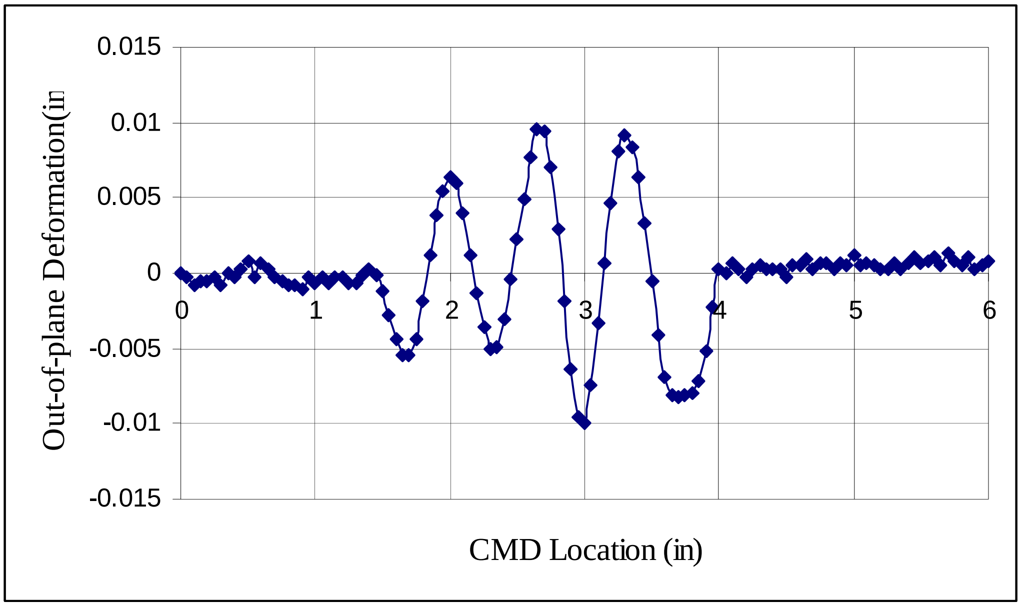

Out-plane-deformation of a 30” test specimen from simulation at a strain of 0.0825

Stretch Test Data:

Thickness(in)	Width(in)	Area(sqin)		Length(in)		Tangent Modulus (psi)
0.0012	10	0.012		600		
Load(pound)	Delta L	L	Strain	Area	Stress	
1	2.375	600	0.00395833	0.012	83.33333	
2	4.5	600	0.0075	0.012	166.6667	
3	6.5625	600	0.0109375	0.012	250	
4	8.875	600	0.01479167	0.012	333.3333	
5	11.25	600	0.01875	0.012	416.6667	
6	13.9375	600	0.02322917	0.012	500	
7	16.9375	600	0.02822917	0.012	583.3333	
8.3	18.31	600	0.03051667	0.012	691.6667	
9	23.4375	600	0.0390625	0.012	750	
10	27.075	600	0.045125	0.012	833.3333	9482.7586
11.1	32.875	600	0.05479167	0.012	925	7500
12	38.875	600	0.06479167	0.012	1000	5673.7589
13	47.6875	600	0.07947917	0.012	1083.333	4705.8824
14	58.3125	600	0.0971875	0.012	1166.667	2203.8567
15	81	600	0.135	0.012	1250	1967.2131
16.2	111.5	600	0.18583333	0.012	1350	1259.8425
17	143.25	600	0.23875	0.012	1416.667	2040.8163
18	167.75	600	0.27958333	0.012	1500	4297.5207
19.3	182.875	600	0.30479167	0.012	1608.333	5276.8284

Poisson’s Ratio Data:

Strain	Poisson's Ratio	Strain	Poisson's Ratio
4.35E-03	0.33	6.52E-02	0.483
4.39E-03	0.329	6.90E-02	0.4734
8.69E-03	0.33	7.41E-02	0.457
8.75E-03	0.329	7.40E-02	0.4638
1.30E-02	0.346	8.26E-02	0.445
1.30E-02	0.33	9.00E-02	0.479
1.74E-02	0.395	9.89E-02	0.472
2.17E-02	0.39	1.02E-01	0.451
2.61E-02	0.385	1.10E-01	0.449
2.70E-02	0.329	1.12E-01	0.454
3.04E-02	0.378	1.20E-01	0.452
3.48E-02	0.38	1.21E-01	0.441
3.98E-02	0.395	1.33E-01	0.448
4.38E-02	0.39	1.34E-01	0.452
4.82E-02	0.4372	1.47E-01	0.467
5.20E-02	0.467	1.47E-01	0.466
5.22E-02	0.443	1.59E-01	0.4779
5.72E-02	0.424	1.60E-01	0.46
6.09E-02	0.4574	1.76E-01	0.4683
6.51E-02	0.4521	1.77E-01	0.44

VITA

Aditya Gotimukul

Candidate for the Degree of

Master of Science

Thesis: Prediction of Amplitude and Wavelengths of Troughs on Polyethylene Webs.

Major Field: Mechanical Engineering

Biographical:

Education:
Completed the requirements for the Master of Science in Mechanical Engineering at Oklahoma State University, Stillwater, Oklahoma in May 2010.

Received Bachelors of Technology in Mechanical Engineering from Jawaharlal Nehru Technological University, Hyderabad, AP, India in May 2007

.

Name: Aditya Gotimukul Date of Degree: May 2010

Institution: Oklahoma State University Location: OKC or Stillwater, Oklahoma

Title of Study: PREDICTION OF AMPLITUDE AND WAVELENGTH OF TROUGHS ON POLYETHYLENE WEBS

Pages in Study: 70 Candidate for the Degree of Master of Science

Major Field: Mechanical Engineering

Scope and Method of Study: Out-of-plane deformations occur in free spans of webs, which may be composed from polymers, during their transportation through process machinery. These troughs may become wrinkles when they transgress a roller. As the amplitudes of these out-of-plane deformations increase the propensity for web wrinkles increase. The goal of this research is to determine if the amplitude and wavelengths of the troughs can be estimated.

Findings and Conclusions: Closed form expressions for amplitude and wavelength of troughs in case of a stretched web were obtained from the literature. Experiments were conducted to stretch the web and measure the out-of-plane deformation. Simulation of troughs formation was done using ABAQUS Explicit. The out-of-plane deformations from both experiments and simulations were obtained at different strain levels for different specimen lengths. Amplitude and wavelength were inferred from the out-of-plane deformations. These amplitudes and wavelengths were compared with the closed form expressions. From the comparisons it was concluded that the wavelength expression was accurate in predicting the wavelengths of the troughs in the elastic and in the inelastic range of the material. The amplitude expressions given by Cerda or developed by Gotimukul are not accurate in predicting the amplitude of the troughs. However these expressions are aids for overestimating the amplitudes of the troughs.

ADVISER'S APPROVAL: Dr. James. K. Good